ORGANOMETALLICS

Article

pubs.acs.org/Organometallics

Potassium and Well-Defined Neutral and Cationic Calcium Fluoroalkoxide Complexes: Structural Features and Reactivity

Sorin-Claudiu Roşca, Thierry Roisnel, Vincent Dorcet, Jean-François Carpentier,* and Yann Sarazin*

Institut des Sciences Chimiques de Rennes, UMR 6226 CNRS, Université de Rennes 1, Campus de Beaulieu, 35042 Rennes Cedex, France

Supporting Information

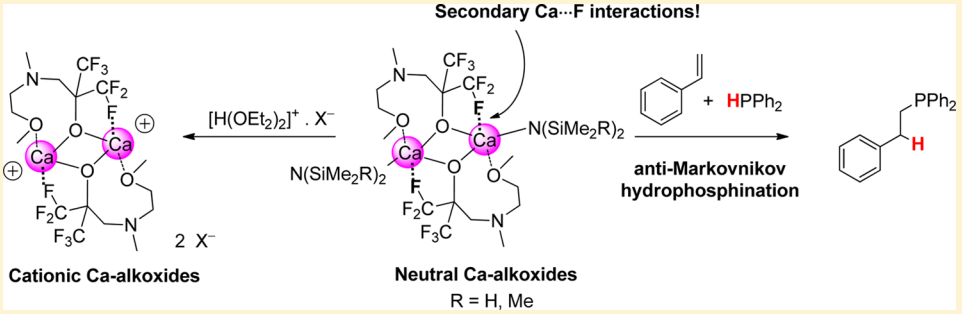

ABSTRACT: The fluorinated aminoether alcohols (1-aza-12-crown-4)$CH_2C(CF_3)_2OH$ ($\{RO_1^F\}H$), $(MeOCH_2CH_2)_2NCH_2C(CF_3)_2OH$ ($\{RO_2^F\}H$), and $(MeOCH_2CH_2)(Me)NCH_2C(CF_3)_2OH$ ($\{RO_3^F\}H$) have been synthesized and used to prepare the heteroleptic calcium amido complexes $\{RO_x^F\}Ca(N(SiMe_2R)_2)$ (**4**–**7**; x = 2, 3, R = H, Me). The ability to form stable complexes varies with the chelating and electron-donating ability of the aminoether alkoxide ligand, as exemplified by our failure to isolate cleanly the elusive $\{RO_1^F\}Ca(N(SiMe_2R)_2)$. X-ray diffraction studies show that, in the solid state, intramolecular Ca···F interactions help reach coordinative saturation in the dimeric $[\{RO_2^F\}Ca(N(SiMe_3)_2)]_2$ ($[\mathbf{4}]_2$), $[\{RO_2^F\}Ca(N(SiMe_2H)_2)]_2$ ($[\mathbf{5}]_2$), $[\{RO_3^F\}Ca(N(SiMe_3)_2)]_2$ ($[\mathbf{6}]_2$), and $[\{RO_3^F\}Ca(N(SiMe_2H)_2)]_2$ ($[\mathbf{7}]_2$), which crystallized free of solvent coligands. Similar stabilizing K···F patterns were found in the polymetallic potassium fluoroalkoxides $[\{RO_1^F\}K]_2$ ($[\mathbf{1}]_2$), $[\{RO_2^F\}K]_4$ ($[\mathbf{2}]_4$), and $[\{RO_3^F\}K]_4$ ($[\mathbf{3}]_4$); $[\mathbf{2}]_4$ and $[\mathbf{3}]_4$ form heterocubanes in the solid state. Examination of the XRD data for $[\mathbf{1}]_2$–$[\mathbf{7}]_2$ shows that metal···F interactions can be favored over binding of O_{ether} atoms for calcium and potassium. Pulse-gradient spin–echo NMR spectroscopy shows that the complexes remain aggregated in aromatic solvents. The solvent-free salts $[\{RO_x^F\}Ca^+]\cdot[H_2N\{B(C_6F_5)_3\}_2^-]$ (x = 1 (**8**), 2 (**9**), 3 (**10**)) are obtained by treating **4**–**7** with $[H(OEt_2)_2^+]\cdot[H_2N\{B(C_6F_5)_3\}_2^-]$ or by reacting $Ca(N(SiMe_3)_2)_2$ with $[\{RO_x^F\}HH^+]\cdot[H_2N\{B(C_6F_5)_3\}_2^-]$; the solid-state structures of $[\mathbf{8}\cdot\mathbf{H_2O}]_2$ and $[\mathbf{9}\cdot\mathbf{H_2O}]_2$ again showed the presence of Ca···F contacts. Complexes **5**–**7** are promising catalysts for the regiospecific anti-Markovnikov hydrophosphination of styrene with diphenylphosphine, affording TOF values as high as 52 mol_{subst} mol_{Ca}^{-1} h^{-1} with up to 400 equiv of substrates within 1–2 h at 60 °C.

INTRODUCTION

Calcium is a large (r_{ionic} = 1.00 Å), electropositive, and oxophilic metal that forms d^0 complexes. Heteroleptic {LX}-$Ca(Nu)(S)_x$ complexes ({LX} = ancillary monoanionic ligand; Nu = monoanionic nucleophile; S = solvent) are of interest for catalysis, but they are labile and readily engage in deleterious Schlenk equilibria. As a result, the coordination chemistry of calcium has been regarded as challenging. Yet, after Hanusa's seminal efforts,[1] it has experienced a surge of interest and synthetic strategies that enable the utilization of calcium complexes for applications in polymerization, fine chemical catalysis, and material science have been devised.[2] Westerhausen has shown that the organometallic chemistry of calcium is diverse and extends further than that of a heavy Grignard analogue.[3] Ruhlandt-Senge has reported low-coordinate [Ca]-amide complexes bearing bulky amides.[4] Not least, the bulky $\{^{Dipp}NacNac\}^-$ ligand (Dipp = diisopropylphenyl) has enabled Roesky[5] and Harder[6] to prepare a collection of heteroleptic $\{^{Dipp}NacNac\}Ca(Nu)(S)_x$ complexes, while Hill used the ubiquitous $\{^{Dipp}NacNac\}Ca(N(SiMe_3)_2)(THF)$ to catalyze a variety of reactions.[2,7] Nevertheless, in spite of these major achievements along with some others,[2] the need for new ligand platforms and routes to robust heteroleptic calcium complexes remains.

In a landmark article, Ruhlandt-Senge discussed that secondary (noncovalent) interactions such as M···C_π, M···N_π, M···F, and agostic bonds are, in some cases, key for the stabilization of alkaline-earth (Ae = Ca, Sr, Ba) complexes.[8] For instance, Ae···H–Si agostic interactions allow the synthesis of

Special Issue: Catalytic and Organometallic Chemistry of Earth-Abundant Metals

Received: March 31, 2014
Published: May 22, 2014

   dx.doi.org/10.1021/om500343w | *Organometallics* 2014, 33, 5630–5642

Chart 1

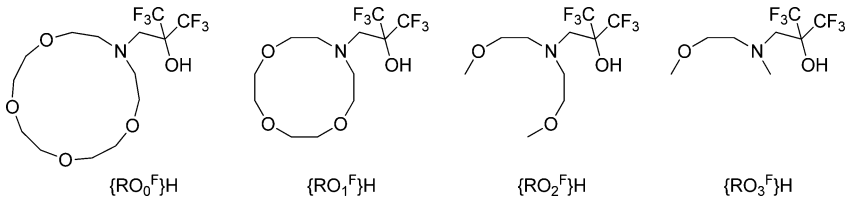

Scheme 1. Synthesis of Potassium (1−3) and Heteroleptic Calcium Amide (4−7) Alkoxides

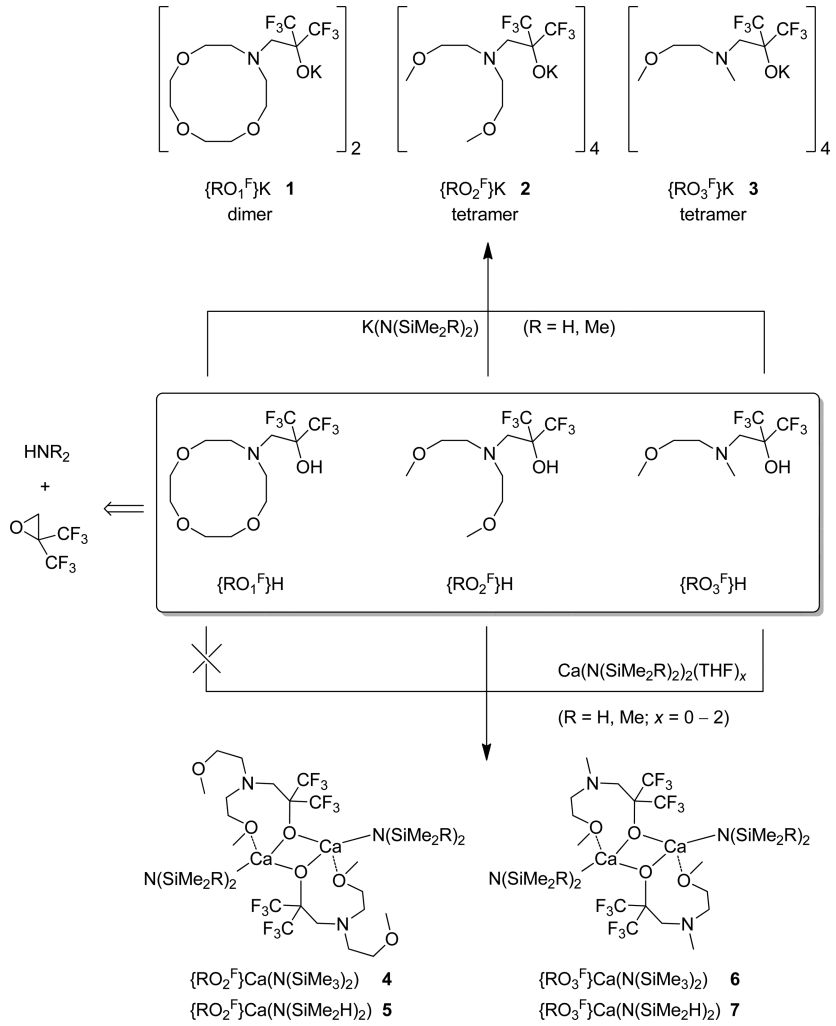

stable $\{LX\}Ae(N(SiMe_2H)_2)(S)_x$ complexes. This strategy has proved valuable to isolate heteroleptic complexes,[9] but the benefits are limited in catalysis, for instance when the $N(SiMe_2H)_2$ amide is replaced by another reactive group prior to entering the catalytic cycle, or because of the intrinsic (detrimental) reactivity of the Si−H moiety.[10] Intramolecular Ae···F interactions between the metal atom and ancillary ligand are attractive, because they are both strong and permanent features of the complex. Fluorinated alkoxide ligands have been used to prepare volatile compounds suitable for metal organic chemical vapor deposition.[11] We have in the past employed fluorinated alkoxo ligands bearing CF_3 groups in positions α to the $O_{alkoxide}$ atom to synthesize group 3, 4, and 13 precatalysts for the polymerization of α-olefins and lactide.[12] These alkoxides are comparable to phenolates in terms of electronic properties, and the steric bulk and electron-withdrawing effect of the α-CF_3 prevent the formation of polymetallic species. Well-defined cationic Ae complexes of the type $[\{RO_0^F\}Ae^+]\cdot[X^-]$, where $\{RO_0^F\}^-$ is a fluorinated alkoxide bearing a 1-aza-15-crown-5 tether and X^- is a weakly coordinating anion, are stable thanks to strong (ca. 30 kcal mol^{-1}) intramolecular Ae··· F interactions,[13] but attempts to prepare the parent charge-neutral $\{RO_0^F\}Ae(N(SiMe_3)_2)$ complexes failed because of kinetic lability, leading to ligand redistribution in solution.

We report here the use of fluorinated alkoxide $\{RO_x^F\}^-$ ligands with aminoether tethers for the synthesis of heteroleptic calcium amide complexes $\{RO_x^F\}Ca(N(SiMe_2R)_2)$ (x = 1−3; R = H, Me; Chart 1). It is shown that Ae···F interactions help toward the stabilization of these species. Their performance as catalysts in the intermolecular hydrophosphination of styrene is illustrated, and their ability to act as precursors for highly electron-deficient $[\{RO_x^F\}Ca^+]\cdot[X^-]$ is presented.

dx.doi.org/10.1021/om500343w | Organometallics 2014, 33, 5630−5642

RESULTS AND DISCUSSION

Synthesis of Potassium and Calcium Charge-Neutral Complexes. The protio ligands $\{RO_x^F\}H$ (prepared in high yields by an equimolar reaction of the appropriate aminoether with 2,2-bis(trifluoromethyl)oxirane)[14,15] react with $KN(SiMe_3)_2$ or $KN(SiMe_2H)_2$ in diethyl ether to afford the corresponding solvent-free potassium salts $\{RO_x^F\}K$ (x = 1 (**1**), 2 (**2**), 3 (**3**)) in satisfactory yields (Scheme 1). Complexes **1**−**3** have been fully characterized; they form a dimer or tetramers in the molecular solid state, and their polymetallic structure persists in solution in aromatic solvents (vide infra). These complexes failed to react cleanly with 1:1 mixtures of CaI_2 and $KN(SiMe_2R)_2$ to give heteroleptic amido calcium complexes during salt metathesis reactions (R = H, Me), and one-pot reactions of $\{RO_x^F\}H$, CaI_2, and 2 equiv of $KN(SiMe_3)_2$ were also unsuitable. Analytically pure samples of the targeted heteroleptic complexes $\{RO_x^F\}Ca(N(SiMe_2R)_2)$ (x = 2, R = Me, **4**; x = 2, R = H, **5**; x = 3, R = Me, **6**; x = 3, R = H, **7**) were eventually obtained in moderate yields by protonolysis of $Ca(N(SiMe_3)_2)_2$, $Ca(N(SiMe_3)_2)_2(THF)_2$, or $Ca(N(SiMe_2H)_2)_2(THF)$ with the suitable protio ligand (Scheme 1). Whereas we anticipated that the protio ligand of highest denticity should also yield heteroleptic complexes, we were unable to obtain $\{RO_1^F\}Ca(N(SiMe_2R)_2)$ for R = H, Me; this was reminiscent of the difficulties encountered in our attempts at making $\{RO_0^F\}Ca(N(SiMe_2R)_2)$.[13] The identities of **4**−**7**, which all form solvent-free bimetallic dimers in the solid state regardless of the nature of the starting material, have been authenticated by structural analysis and NMR spectroscopy, and their purity was corroborated by combustion analyses. Complexes **5**−**7** are soluble in common nonprotic organic solvents (ethers, hydrocarbons) and decompose within minutes in chlorinated solvents (CD_2Cl_2, $CDCl_3$). Their NMR data were recorded in benzene-d_6; **4** is only sparingly soluble in hydrocarbons, and THF-d_8 was used as the NMR solvent.

The hexamethyldisilazide compounds **4** and to a lesser extent **6** are less stable than the congeneric tetramethyldisilazides **5** and **7**; in particular, **4** rapidly shows signs of decomposition in solution. This was tentatively attributed to the presence of stabilizing Ca···H−Si interactions in **5** and **7**, although their existence could not be firmly demonstrated by spectroscopic methods.

The $^{19}F\{^1H\}$ NMR spectra for the potassium complexes **1**−**3** and the calcium complexes **4** and **5** exhibit a single, sharp singlet for the CF_3 groups typically in the range $\delta_{^{19}F}$ −77.2 to −81.8 ppm, indicating the equivalence of all CF_3 moieties in solution for these complexes. On the other hand, two quartets of equal intensity are detected in the spectra of the Ca complexes **6** (centered at −73.4 and −75.1 ppm; $^4J_{FF}$ = 9.4 Hz) and **7** (centered at −76.5 and −76.8 ppm; $^4J_{FF}$ = 9.4 Hz), indicating that the CF_3 groups are in these cases nonequivalent. Hence, the $^{19}F\{^1H\}$ NMR spectra for **1**−**7** recorded at 25 °C provided no evidence for the metal···F intramolecular interactions detected in all these complexes in the molecular solid state (vide infra). Attempts to observe splitting of the resonances by recording low-temperature data (down to −80 °C) did not improve on this situation; evidently the CF_3 groups are highly fluxional, rotating and exchanging positions too easily for NMR detection methods. In their ^1H NMR spectra, complexes **5** and **7** exhibit a resonance at $\delta_{^1H}$ 4.88 and 4.86 ppm, respectively, assigned to the Si*H* moieties. These chemical shifts and the corresponding $^1J_{SiH}$ coupling constant (162 Hz in both cases) do not provide compelling evidence for the presence of intramolecular Ca···H−Si interactions; again, low-temperature NMR brought no improvement, and decoalescence of the resonance that could potentially be expected did not occur at −80 °C. Consistent with this, the FTIR spectra of **5** and **7** show a unique, symmetric absorption band for Si−H stretching at $\tilde{\nu}$ 2016 and 2015 cm^{-1}, i.e. in the region expected for Si*H* moieties *not* interacting with a metal center; Ae···H−Si contacts (Ae = Ca−Ba) are characterized by a band at lower energy, typically 1900−1980 cm^{-1}, depending on the strength of the interaction and identity of the metal. The $^{29}Si\{^1H\}$ NMR data for **5** and **7** ($\delta_{^{29}Si}$ −25.1 and −25.4 ppm, respectively) are comparable to those for related $\{LO\}Ca(N(SiMe_2H)_2)(THF)_x$ aminoether phenolate complexes.[9]

Solid-State Structural Investigations. Single crystals of **1**−**7** were grown typically from concentrated hydrocarbon (toluene, benzene, and/or pentane) or diethyl ether solutions, and their structures were determined by X-ray diffraction studies.

The complex $\{RO_1^F\}K$ (**1**) recrystallized as the centrosymmetric dimer $[\mathbf{1}]_2$, where each metal atom is 8-coordinated and the two K atoms are directly bridged through the $O_{alkoxide}$ atoms (Figure 1). The coordination sphere on each metal is completed by the four heteroelements from the macrocyclic tether and by two fluorine atoms situated at a short distance from the metals (average K···F = 2.98 Å). These F···K contacts fall in the same range as those reported for $K[Cu(OC_4F_9)_2]$ complexes (average distance K···F = 2.96 Å),[16] for the $K(18\text{-crown-6})^+$ salt of germanium fluorinated pentoxide (K···F = 3.02 and 3.28 Å),[17] and for heteropolymetallic $[KM(OC(CF_3)_3)_3(THF)]_4$ compounds used for MOCVD (M = Sr, average K···F = 2.94 Å; M = Ba, average K···F = 3.04 Å ; M = Eu; average K···F = 2.95 Å).[11b] In addition to the bridging $O_{alkoxide}$, each fluorinated alkoxide dispenses one K···F contact

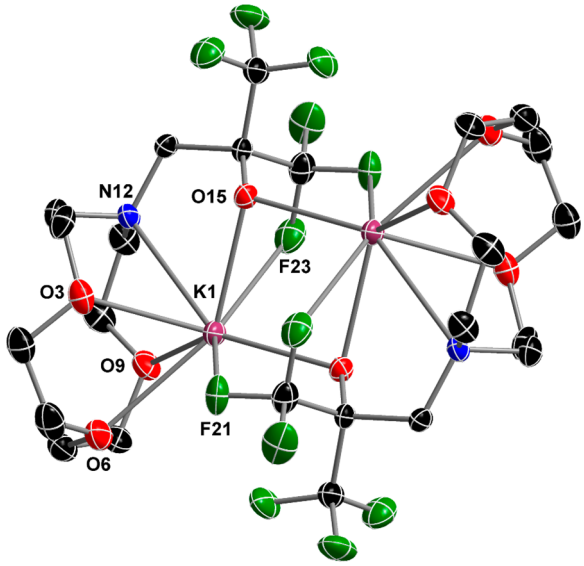

Figure 1. ORTEP representation of the molecular structure of $\{RO_1^F\}K$ (**1**), recrystallized as the centrosymmetric dimer $[\mathbf{1}]_2$. Hydrogen atoms are omitted for clarity. Ellipsoids are drawn at the 50% probability level. Selected bond lengths (Å) and angles (deg): K(1)−O(15) = 2.630(2), K(1)−O(15)$^{\#1}$ = 2.682(2), K(1)−O(3) = 2.777(2), K(1)−O(6) = 2.821(2), K(1)−O(9) = 2.753(2), K(1)−N(12) = 2.990(2), K(1)−F(21)$^{\#1}$ = 2.928(2), K(1)−F(23) = 3.035(2), K(1)−K(1)$^{\#1}$ = 3.842(1); K(1)−O(15)−K(1)$^{\#1}$ = 92.65(5).

dx.doi.org/10.1021/om500343w | *Organometallics* 2014, 33, 5630−5642

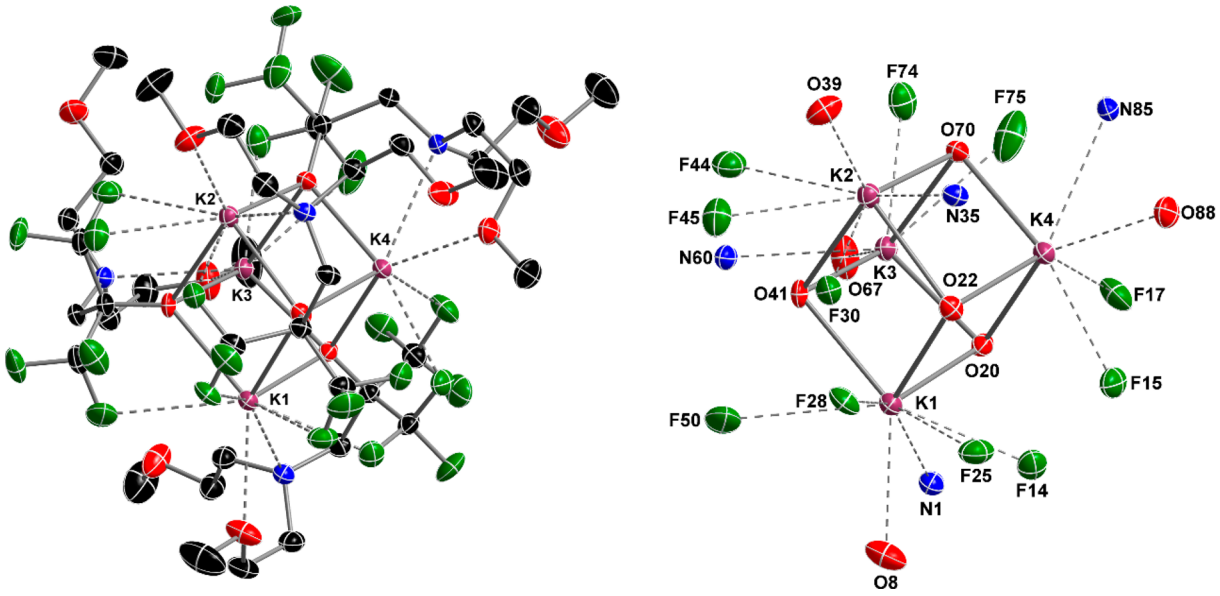

Figure 2. (left) ORTEP representation of the molecular structure of $\{RO_2^F\}K$ (**2**), recrystallized as the tetramer $[\mathbf{2}]_4$. Hydrogen atoms are omitted for clarity. (right) Simplified representation of the K_4O_4 heterocubane in $[\mathbf{2}]_4$, showing the coordination sphere around K atoms and the atom-numbering scheme. Color scheme: F atoms, green; K atoms, purple; C atoms, black; O atoms, red; N atoms, blue. Ellipsoids are drawn at the 50% probability level. Selected bond lengths (Å): K(1)−O(8) = 2.815(2), K(1)−O(20) = 2.642(1), K(1)−O(22) = 2.707(1), K(1)−O(41) = 2.707(1), K(1)−F(14) = 2.879(1), K(1)−F(25) = 3.076(1), K(1)−F(28) = 2.862(1), K(1)−F(50) = 3.155(1), K(1)−N(1) = 3.060(2), K(2)−O(22) = 2.639(1), K(2)−O(39) = 2.777(1), K(2)−O(41) = 2.800(1), K(2)−O(70) = 2.699(1), K(2)−F(30) = 2.830(1), K(2)−F(44) = 3.138(1), K(2)−F(45) = 2.857(1), K(2)−N(35) = 2.979(2), K(3)−O(20) = 2.627(1), K(3)−O(41) = 2.620(1), K(3)−O(67) = 2.738(2), K(3)−O(70) = 2.775(1), K(3)−F(74) = 2.865(1), K(3)−F(75) = 3.238(2), K(3)−N(60) = 3.060(2), K(4)−O(20) = 2.692(1), K(4)−O(22) = 2.634(1), K(4)−O(70) = 2.599(1), K(4)−O(88) = 2.708(2), K(4)−F(15) = 2.761(1), K(4)−F(17) = 2.962(1), K(4)−N(85) = 2.974(12).

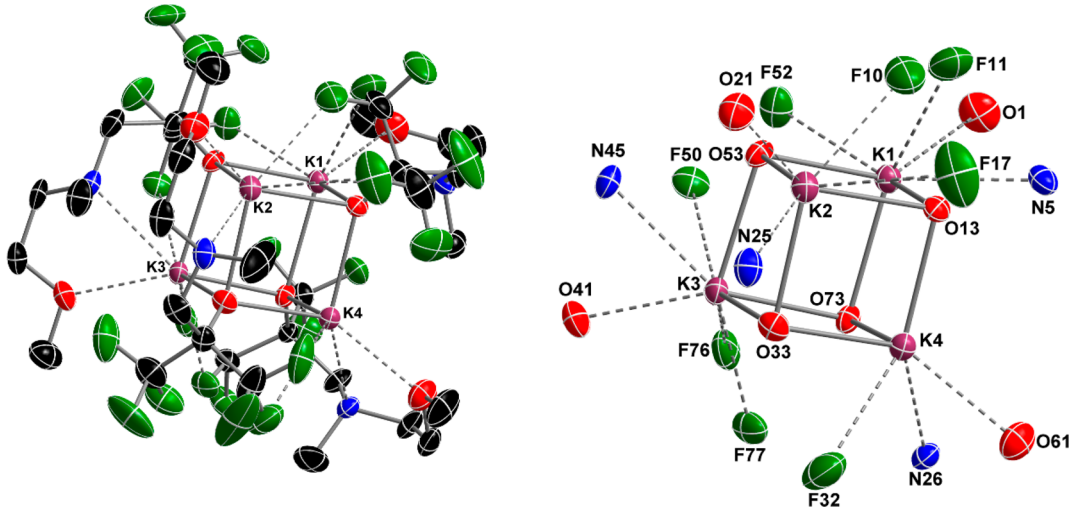

Figure 3. (left) ORTEP representation of the molecular structure of $\{RO_3^F\}K$ (**3**), recrystallized as the tetramer $[\mathbf{3}]_4$. Only one of the two independent and comparable molecules found in the asymmetric unit is depicted. Hydrogen atoms are omitted for clarity. (right) Simplified representation of the K_4O_4 heterocubane in $[\mathbf{3}]_4$, showing the coordination sphere around K atoms and the atom-numbering scheme. Color scheme: F atoms, green; K atoms, purple; C atoms, black; O atoms, red; N atoms, blue. Ellipsoids are drawn at the 50% probability level. Selected bond lengths (Å): K(1)−O(1) = 2.774(6), K(1)−O(13) = 2.666(5), K(1)−O(53) = 2.709(5), K(1)−O(73) = 2.708(5), K(1)−N(5) = 2.911(7), K(1)−F(11) = 2.908(7), K(1)−F(52) = 2.839(5), O(13)−K(2) = 2.744(5), K(2)−O(21) = 2.810(6), K(2)−O(33) = 2.658(5), K(2)−O(53) = 2.643(5), K(2)−N(25) = 2.910(7), F(10)−K(2) = 2.777(6), F(17)−K(2) = 3.180(7), O(33)−K(3) = 2.699(5), K(3)−O(41) = 2.734(5), K(3)−O(53) = 2.677(5), K(3)−O(73) = 2.739(5), K(3)−N(45) = 2.875(6), K(3)−F(50) = 2.923(5), K(3)−F(77) = 2.931(5), K(3)−F(76) = 3.011(6), O(13)−K(4) = 2.635(5), O(33)−K(4) = 2.681(5), K(4)−O(61) = 2.765(6), K(4)−O(73) = 2.623(5), K(4)−N(26) = 2.921(6), F(30)−K(4) = 3.020(7), F(32)−K(4) = 3.081(7), K(1)−K(4) = 3.786(2), K(2)−K(3) = 3.710(2), K(2)−K(4) = 3.767(2).

with each of the metal atoms, and therefore they both act overall as a μ_2:κ^6,κ^2 chelate. The K(1)···K(1)$^{\#1}$ distance of 3.84 Å is much shorter than that in elemental potassium (4.54 Å) and smaller than double the van der Waals radius of potassium (r_{vdW} = 2.75 Å); this coincides with a narrow K(1)−O(15)−K(1)$^{\#1}$ angle of 92.6°. Similar or even stronger geometric constraints were for instance seen in the complex $K_2Ru_2(Co)_4(PPh_3)_2(4\text{-}t\text{Bu-}C_6H_5O)_6$ (K···K = 3.60 Å, ∠(K−O−K) = 78.3°),[18] in the potassium calix[4]arene complex $\{[calix[4](O)_4K]_2(\mu\text{-}K)_6(THF)_{10}\}$ (K···K = 3.27 Å, ∠(K−O−

dx.doi.org/10.1021/om500343w | *Organometallics* 2014, 33, 5630−5642

K) = 75.6°),[19] and in $[\{RO_0^F\}K]_2$ (K···K = 3.68 Å, ∠(K−O−K) = 89.3°).

The complex $\{RO_2^F\}K$ (**2**) recrystallized as the tetramer $[\mathbf{2}]_4$, with a central K_4O_4 core adopting a slightly distorted cubic arrangement where each metal atom is adjacent to three $O_{alkoxide}$ atoms (Figure 2). The formation of heterocubanes is well-known for alkali-metal alkoxides, as for instance seen in $[MOC_4F_9]_4$ (M = Na, K).[20] Each metal atom engages in two to four nonequivalent K···F interactions with neighboring CF_3 groups (average distance K···F (Å): K(1), 2.99; K(2), 2.94; K(3), 3.05; K(4), 2.86; the limit for significant K···F interactions was set at 3.23 Å),[21] and the coordination sphere is completed by the $N_{side\ arm}$ atom and *only one* $O_{side\ arm}$ atom, with total coordination numbers varying from 7 to 9. The other metric parameters around the metals in $[\mathbf{2}]_4$ are unexceptional. Note that, for each metal, the binding of only one of the two OMe moieties in the aminoether tether is required to ensure coordinative saturation, as the addition of multiple K···F interactions turns out to be more stabilizing than the coordination of the second OMe, a possibility already suggested by Ruhlandt-Senge.[8a] As a matter of fact, the second methoxy does not interact with any metal atom in the crystal lattice, and the coordination spheres about the metal atoms in $[\mathbf{2}]_4$ actually resemble closely those in $[\mathbf{3}]_4$, also a heterocubane obtained upon recrystallization of $\{RO_3^F\}K$ (**2**) where the dangling CH_2CH_2OMe fragment is replaced by a simple methyl group on the N atom (Figure 3). The heterocubane structure imposes short K···K distances (ca. 3.60−4.00 Å) and narrow K−O−K angles in these two complexes. Formation of tetramers $[\mathbf{2}]_4$ and $[\mathbf{3}]_4$ with the ligands $\{RO_2^F\}$ and $\{RO_3^F\}$, in contrast to the dimer seen with $\{RO_1^F\}$ in $[\mathbf{1}]_2$ (and with $\{RO_0^F\}$),[21] can be linked to the lower intrinsic coordinating ability of these ligands.

The molecular structure of the dimeric calcium complex $[\mathbf{5}]_2$ depicted in Figure 4 shows a peculiar arrangement about the metal atoms. The positions of the Si*H* hydrogen atoms were not idealized but were determined from the electron density map. In this dimer, which features an inversion center, the metal atoms are 6-coordinated or, if Ca···H−Si is taken into account, 7-coordinated. The large discrepancies between the two Ca−N−Si angles (103.3 and 126.7°) and corresponding Ca···Si distances (3.15 and 3.58 Å to Si(1) and Si(2), respectively) indeed suggest that the Si(1)−H(1S) moieties are involved in agostic bonding with the metal atoms. The coplanarity of Ca(1)−N(1)−Si(1)−H(1S) is in agreement with this interpretation.[9] Yet, one may also note that Si(2) and H(2S) also fit in this very plane, even if other metric parameters do not support the claim of Ca···H(2S)−Si(2) agostic interactions. Pertinent metric parameters for $[\mathbf{5}]_2$ and other related calcium complexes are collected in Table 1.

The structural features presented here may indeed argue in favor of (at least) Ca···H(1S)−Si(1) agostic bonding, but spectroscopic methods did not provide supporting evidence (vide supra), and we are unable to conclude as to the existence of such agostic bonding on the basis of these experimental data. There is no ambiguity regarding the Ca(1)···F(14) interaction[22] characterized by a short distance of 2.83 Å between these two atoms, even if the intensity of this secondary interaction is weaker than that detected in $\{^{Dipp}NacNac_{(CF3)2}\}$-$Ca(N(SiMe_3)_2)(THF)_2$ (Ca···F = 2.47 and 2.49 Å)[23] and in the cationic complex $[\{RO_0^F\}Ae^+]\cdot[H_2N\{B(C_6F_5)_3\}_2^-]$ (Ca···F = 2.64−2.68 Å).[13] Expectedly, the Ca−N_{amide} (2.31 Å) bond length is much shorter than the Ca−N_{amine} length (2.60 Å),

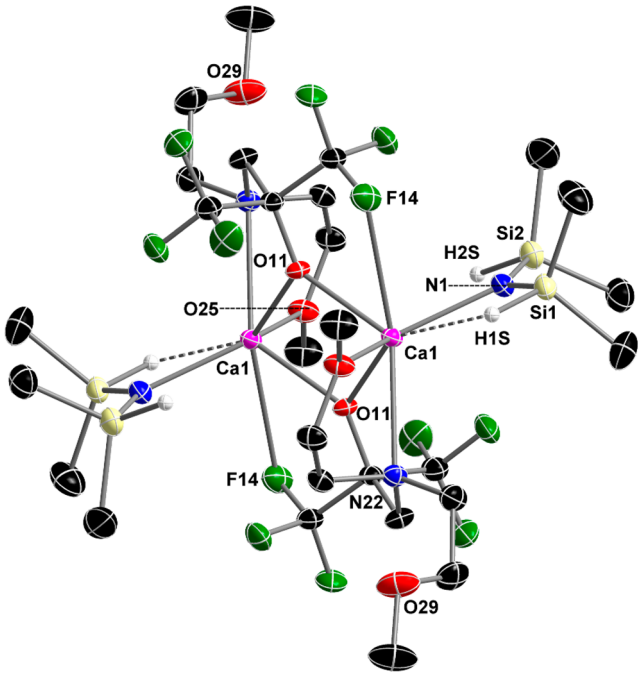

Figure 4. ORTEP representation of the molecular structure of $[\{RO_2^F\}Ca(N(SiMe_2H)_2)]_2$ ($[\mathbf{5}]_2$). Hydrogen atoms (except Si*H*) are omitted for clarity. Ellipsoids are drawn at the 50% probability level. Selected bond lengths (Å) and angles (deg): Ca(1)−O(11) = 2.295(1), Ca(1)−$O(11)^{\#1}$ = 2.302(1), Ca(1)−N(1) = 2.310(1), Ca(1)−$O(25)^{\#1}$ = 2.419(1), Ca(1)−$N(22)^{\#1}$ = 2.597(1), Ca(1)−F(14) = 2.833(1); Si(1)−N(1)−Ca(1) = 103.27(7), Si(2)−N(1)−Ca(1) = 126.68(8), Ca(1)−O(11)−$Ca(1)^{\#1}$ = 104.63(4), Si(1)−N(1)−Si(2) = 130.03(9).

whereas the bridging $O_{alkoxide}$ atoms are also substantially closer to the metal atoms (ca. 2.30 Å) than the sole $O_{methoxy}$ atom involved in the coordination sphere of the metal (Ca(1)−O(25) = 2.42 Å). Remarkably, in line with the above observations on $[\mathbf{2}]_4$, the other methoxy side arm (viz. O(29)) in $[\mathbf{5}]_2$ does not interact with any metal atom, as coordinative saturation is filled by the $N(SiMe_2H)_2$ moiety and a Ca···F secondary interaction in addition to the ancillary ligand.

The geometry in the centrosymmetric dimer $[\mathbf{4}]_2$ (Figure 5) is similar to that in $[\mathbf{5}]_2$ (Table 1), except that the potential Ca···H−Si agostic interaction in the latter in now replaced by a second, albeit weaker, Ca···F contact. The metal atoms in $[\mathbf{4}]_2$ are 7-coordinated, with relatively intense (Ca···F(20) = 2.92 Å) and loose (Ca···F(15) = 3.11 Å) secondary interactions, while the rest of the coordination sphere is occupied by the ancillary ligand. The metric parameters about the metal in $[\mathbf{4}]_2$ are comparable to those measured in $[\mathbf{5}]_2$, and again one of the $O_{methoxy}$ atoms (viz. O(25)) is not interacting with the metal atoms. On the other hand, the geometric features around the N_{amide} atoms are different; the Si−N−Si angle of 121.5° is narrower than that in $[\mathbf{5}]_2$ (130.0°), and the difference between the two types of Ca−N−Si angles in $[\mathbf{4}]_2$ (112.5 and 125.6°) is not as great as in $[\mathbf{5}]_2$. These observations, as well as the coordination of a second F atom to achieve a coordination number of 7, seem to militate in favor of a Ca···H−Si agostic interaction in $[\mathbf{5}]_2$ in the solid state.

The bonding pattern in the centrosymmetric dimer $[\{RO_3^F\}$-$CaN(SiMe_2H)_2]_2$ ($[\mathbf{7}]_2$) matches that in $[\mathbf{5}]_2$, except for the fact that the dangling, noncoordinating CH_2CH_2OMe side arm

dx.doi.org/10.1021/om500343w | *Organometallics* 2014, 33, 5630−5642

Table 1. Summary of Metric Data for the Heteroleptic Calcium Complexes $[4]_2$–$[7]_2$

complex	Ca atom	Ca···F (Å)	Ca···Si (Å)	Ca–N–Si (deg)	N–Si–N (deg)
$[\{RO_2^F\}Ca(N(SiMe_3)_2)]_2$ ($[4]_2$)	Ca(1) = Ca(1)$^{\#1}$	2.92	3.37	112.5	121.5
		3.11	3.60	125.6	
$[\{RO_2^F\}Ca(N(SiMe_2H)_2)]_2$ ($[5]_2$)	Ca(1) = Ca(1)$^{\#1}$	2.83	3.15	103.3	130.0
			3.58	126.7	
$[\{RO_3^F\}Ca(N(SiMe_3)_2)]_2$ ($[6]_2$)	Ca(1)	3.08	3.42	114.4	119.7
			3.62	125.2	
	Ca(2)	2.71	3.35	109.9	121.6
		3.06	3.65	128.0	
$[\{RO_3^F\}Ca(N(SiMe_2H)_2)]_2$ ($[7]_2$)	Ca(1) = Ca(1)$^{\#1}$	3.00	3.29	110.8	128.2
			3.47	120.5	

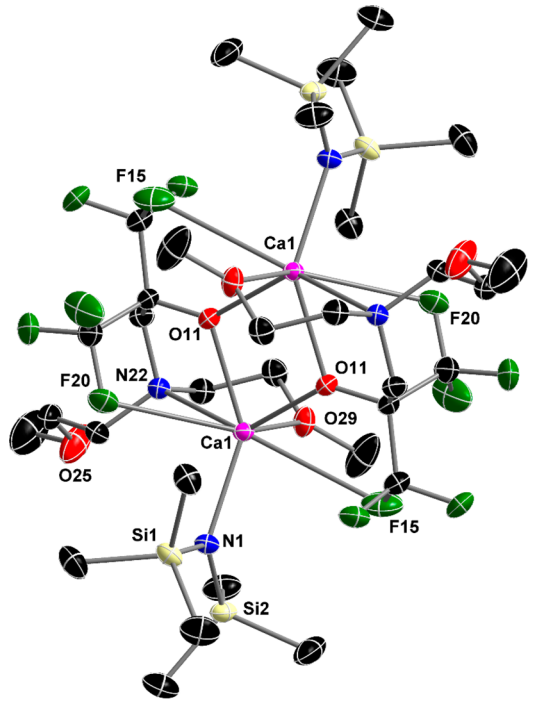

Figure 5. ORTEP representation of the molecular structure of $[\{RO_2^F\}Ca(N(SiMe_3)_2)]_2$ ($[4]_2$). Hydrogen atoms are omitted for clarity. Ellipsoids are drawn at the 50% probability level. Selected bond lengths (Å) and angles (deg): Ca(1)–O(11) = 2.332(1), Ca(1)–N(1) = 2.332(1), Ca(1)–F(15) = 3.113(2), Ca(1)–O(11)$^{\#1}$ = 2.343(1), Ca(1)–O(29)$^{\#1}$ = 2.375(1), Ca(1)–N(22)$^{\#1}$ = 2.719(2), Ca(1)–F(20)$^{\#1}$ = 2.920(1); Si(1)–N(1)–Si(2) = 121.48(9), Si(1)–N(1)–Ca(1) = 112.46(7), Si(2)–N(1)–Ca(1) = 125.64(8), Ca(1)–O(11)–Ca(1)$^{\#1}$ = 105.64(5).

that was in $[5]_2$ has now been replaced by a simple methyl group. As can be seen in Figure 6 and in Table 1, this bears no incidence on the coordination about the metal atoms. There is one Ca···F secondary interaction for each metal in $[7]_2$, with a corresponding distance of 3.00 Å.

The arrangement is different in $[\{RO_3^F\}Ca(N(SiMe_3)_2)]_2$ ($[6]_2$), displayed in Figure 7. Here, the two calcium atoms are not equivalent (Table 1). The atom Ca(1) is 6-coordinated, having only one Ca···F interaction (with F(26), 3.08 Å); the atom Ca(2) is 7-coordinated as found in $[4]_2$, with two Ca···F contacts of 2.71 and 3.06 Å. The Ca_2O_2 central core is not symmetrical, and the interaction of a single F atom on Ca(1) generally induces slight deviations from symmetry throughout the dimer. Note, however, that the values of the two N–Si–N angles are very close.

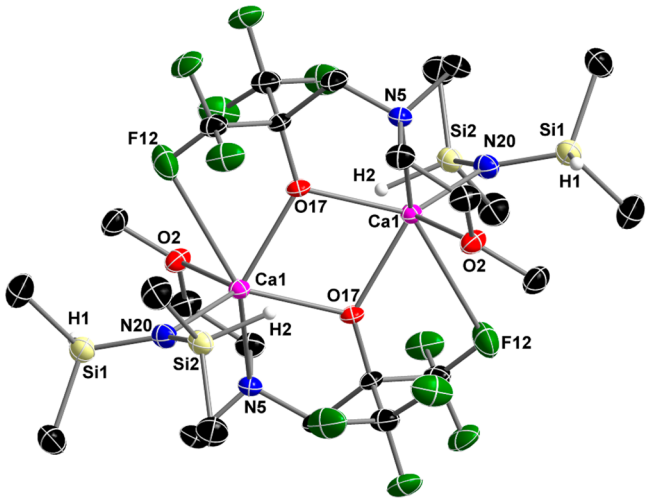

Figure 6. ORTEP representation of the molecular structure of $[\{RO_3^F\}Ca(N(SiMe_2H)_2)]_2$ ($[7]_2$). Hydrogen atoms (except Si*H*, the position of which was accurately localized from the electron density map) are omitted for clarity. Ellipsoids are drawn at the 50% probability level. Selected bond lengths (Å) and angles (deg): Ca(1)–N(20) = 2.300(1), Ca(1)–O(17) = 2.311(1), Ca(1)–O(17)$^{\#1}$ = 2.318(1), Ca(1)–O(2) = 2.408(1), Ca(1)–N(5) = 2.571(1), Ca(1)–F(12)$^{\#1}$ = 3.005(1); Si(2)–N(20)–Si(1) = 128.16(8), Si(2)–N(20)–Ca(1) = 110.83(6), Si(1)–N(20)–Ca(1) = 120.49(7), Ca(1)–O(17)–Ca(1)$^{\#1}$ = 105.03(4).

NMR Diffusion Measurement Experiments. The nuclearity of the potassium complexes **2** and **3** and calcium complexes **4**–**7** in solution was assessed by pulse gradient spin–echo (PGSE) NMR spectroscopy, following protocols developed for related alkaline and alkaline-earth complexes.[24] All measurements were performed at 298 K, using 13.0–30.0 mM solutions in benzene-d_6.[25] The validity of the method was assessed using $Si(SiMe_3)_4$ (TMSS) as a reference. From the PGSE experiments, the translational coefficient D_t was acquired for all compounds from the plot of $\ln(I/I_0)$ vs $-\gamma^2\delta^2G^2(\Delta - \delta/3)D_t$ (see the Experimental Section for details). The values of the hydrodynamic radius of the metal complexes ($r_{H,PGSE}$) thus determined are collected in Table 2.[26] For all complexes, the value of the hydrodynamic radius determined from the solid-state structures (ellipsoidal model)[24] matches well that estimated by PGSE experiments, suggesting that they maintain their polynuclear structure in aromatic hydrocarbons.

These measurements also confirmed that the heteroleptic complexes $[\{RO_x^F\}Ca(N(SiMe_2R)_2)]_2$ (R = H, Me) do not decompose entirely or in part to a mixture of homoleptic

dx.doi.org/10.1021/om500343w | Organometallics 2014, 33, 5630–5642

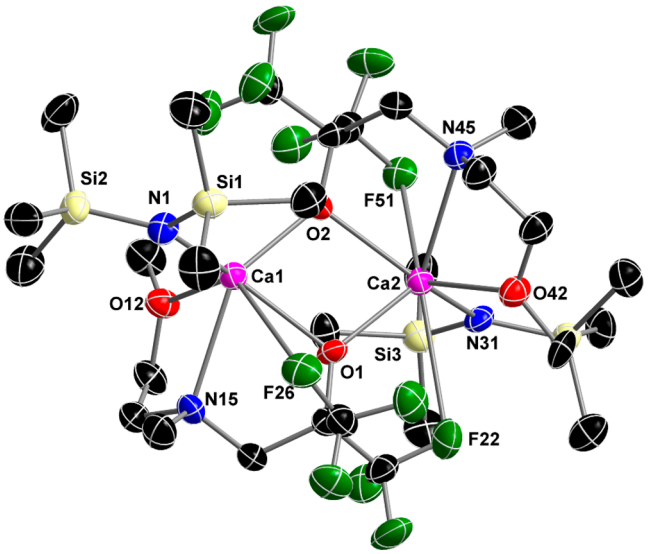

Figure 7. ORTEP representation of the molecular structure of $[\{RO_3^F\}Ca(N(SiMe_3)_2)]_2$ ($[\mathbf{6}]_2$). Hydrogen atoms and noninteracting benzene molecules are omitted for clarity. Ellipsoids are drawn at the 50% probability level. Selected bond lengths (Å) and angles (deg): Ca(1)−O(2) = 2.305(5), Ca(1)−N(1) = 2.353(7), Ca(1)−O(1) = 2.371(5), Ca(1)−O(12) = 2.397(6), Ca(1)−N(15) = 2.615(7), Ca(1)−F(26) = 3.084(6), Ca(1)−Ca(2) = 3.760(2), O(1)−Ca(2) = 2.317(5), O(2)−Ca(2) = 2.403(5), F(22)−Ca(2) = 3.056(6), Ca(2)−N(31) = 2.370(7), Ca(2)−O(42) = 2.475(6), Ca(2)−N(45) = 2.627(7), Ca(2)−F(51) = 2.712(5); Si(4)−N(31)−Si(3) = 121.6(4), Si(1)−N(1)−Si(2) = 119.7(4).

species $\{RO_x^F\}_2Ca$ and $Ca(N(SiMe_3)_2)_2$, as a single diffusion coefficient was measured in all cases.[27]

Bond Valence Analysis. The contribution of secondary interactions (K···F and Ca···F) to the coordination sphere of the metal atoms can be estimated using bond valence sum analysis (BVSA). This theoretical model, first introduced by Brown and Altermatt[28] and later developed by O'Keefe and Brese,[29] makes use of bond distances obtained from single-crystal X-ray diffraction to assign the contribution of each neighboring atom toward the metallic center through traditional interactions and secondary interactions. Bond valences (ν) were calculated for each environment in the complexes $[\{RO_2^F\}K]_4$ ($[\mathbf{2}]_4$) and $[\{RO_2^F\}Ca(N(SiMe_3)_2)]_2$ ($[\mathbf{4}]_2$) using eq 1, with experimental bond lengths d_{Met-X} and tabulated bond lengths R_{Met-X}:

$$\nu = \exp[(R_{Met-X} - d_{Met-X})/B] \quad (1)$$

where X = O, F, N; Met = K, Ca; B = 0.37; R_{K-O} = 2.132, R_{K-F} = 1.992, R_{K-N} = 2.260; R_{Ca-O} = 1.967, R_{Ca-F} = 1.842, R_{Ca-N} = 2.140.[28,29]

For the calcium complex $[\mathbf{4}]_2$ (Table 3), coordinative saturation is not reached if only coordination of the N and O side atoms is considered. Further extension by inclusion of the Ca···F interactions affords near coordinative saturation ($\sum\nu$ = 1.959), and in this case the mean contribution of Ca···F interactions to the overall coordination sphere approaches 4%.

For $[\mathbf{2}]_4$, the mean contribution of K···F interactions to the coordination sphere (averaged over the four metal atoms) amounted to a considerable 18% (see the Supporting Information). This value compares well with the average values determined for $[\{RO_3^F\}K]_4$ ($[\mathbf{3}]_4$) (17%; see the Supporting Information) and Ruhlandt-Senge's $[K(PFTB)(THF)_4]$ (20%; PFTB = perfluoro-*tert*-butoxide).[11b] Higher K···F contributions were found in the tetrameric alkoxides $KOC(Ph)(CF_3)_2$ (34%) and $KOCMe(CF_3)_2$ (32%), respectively,[30] which is unsurprising, as the K atoms are not supported by side N/O atoms in these compounds.

Synthesis of Calcium Cations. Cationic calcium complexes devoid of coordinated solvent are rare because of their intrinsic sensitivity, but they present an interest in catalysis owing to their high electrophilicity.[13] The compounds $[\{RO_1^F\}Ca^+]\cdot[H_2N\{B(C_6F_5)_3\}_2^-]$ (**8**), $[\{RO_2^F\}Ca^+]\cdot[H_2N\{B(C_6F_5)_3\}_2^-]$ (**9**), and $[\{RO_3^F\}Ca^+]\cdot H_2N\{B(C_6F_5)_3\}_2^-]$ (**10**) were obtained as colorless solids by equimolar reactions of $Ca(N(SiMe_3)_2)_2$ with the appropriate doubly acidic compounds $[\{RO_x^F\}HH^+]\cdot[H_2N\{B(C_6F_5)_3\}_2^-]$ (x = 1−3; these are prepared by treatment of $\{RO_x^F\}H$ with Bochmann's acid, $[H(OEt_2)_2\}^+]\cdot[H_2N\{B(C_6F_5)_3\}_2^-]$;[31] see the Supporting Information) in chlorobenzene (Scheme 2). Solvents such as THF must be avoided because of the risk of coordination onto the metal, and hence the standard synthetic precursor $Ca(N(SiMe_3)_2)_2(THF)_2$ should not be used. Alternatively, **9** and **10** were also prepared by addition of Bochmann's acid to **5** and **6**, respectively, but this is less convenient, as it entails the preliminary synthesis of the charge-neutral heteroleptic parent complexes. The choice of the counterion $H_2N\{B(C_6F_5)_3\}_2^-$ was prompted by synthetic considerations. This large (538 Å^3),[32] weakly coordinating anion possesses a dipolar moment which provides good crystallization properties, and indeed salts of this anion are known to crystallize more easily than with the spherical, more conventional $B(C_6F_5)_4^-$ borate derivative.[33]

The compositions of **8**−**10** were authenticated by NMR spectroscopy, and their purity was confirmed by microanalytical measurements. They are poorly soluble in nonpolar solvents,

Table 2. PGSE NMR Measurements and X-ray Crystallographic Data for Complexes 2−7[a]

complex	D_t[b] (10^{-9} m^2 s^{-1})	$r_{H,PGSE}$ (Å)	X-ray a (Å)	X-ray b (Å)	$r_{H,X\text{-}ray}$[c] (Å)
$[\{RO_2^F\}K]_4$ ($[\mathbf{2}]_4$)	0.88	5.74	7.65	4.65	6.48
$[\{RO_3^F\}K]_4$ ($[\mathbf{3}]_4$)	0.77	6.45	5.59	5.23	5.47
$[\{RO_2^F\}Ca(N(SiMe_3)_2)]_2$ ($[\mathbf{4}]_2$)	1.33	5.25	6.93	4.48	5.99
$[\{RO_3^F\}Ca(N(SiMe_3)_2)]_2$ ($[\mathbf{6}]_2$)	1.13	6.01	6.95	4.87	6.17
$[\{RO_2^F\}Ca(N(SiMe_2H)_2)]_2$ ($[\mathbf{5}]_2$)	0.65	6.14	7.60	4.78	6.51
$[\{RO_3^F\}Ca(N(SiMe_2H)_2)]_2$ ($[\mathbf{7}]_2$)	1.49	4.75	5.56	4.68	5.25

[a]All NMR spectra were recorded in C_6D_6 at 298 K using 13.0−30.0 mM solutions of complex and of the external reference $Si(SiMe_3)_4$ (TMSS). [b]Average of the values of D_t found for three or more separate peaks in the ^{1}H PGSE NMR spectrum of the complex. [c]Calculated according to $r_{H,X\text{-}ray} = (a^2b)^{1/3}$ where a and b, respectively, the major and minor semiaxes of the prolate ellipsoid formed by the complex, are determined from the solid-state structures.

dx.doi.org/10.1021/om500343w | *Organometallics* 2014, 33, 5630−5642

Table 3. Bond Valence Analysis Calculations for $[\{RO_2^F\}Ca(N(SiMe_3)_2)]_2$ ($[\mathbf{4}]_2$; Met = Ca(1))

d(Ca–O)[a]	d(Ca–F)[a]	d(Ca–N)[a]	ν(Ca–O)[b]	ν(Ca–F)[b]	ν(Ca–N)[b]	$\sum\nu$
2.331	2.920	2.332	0.374	0.054	0.595	
2.343	3.110	2.719	0.362	0.032	0.209	
2.374			0.333			
			1.069	0.086	0.804	1.959

[a]Data from the X-ray structure of $[\mathbf{4}]_2$. [b]Calculated using eq 1.

Scheme 2. Synthesis of Cationic Calcium Fluoroalkoxide Complexes

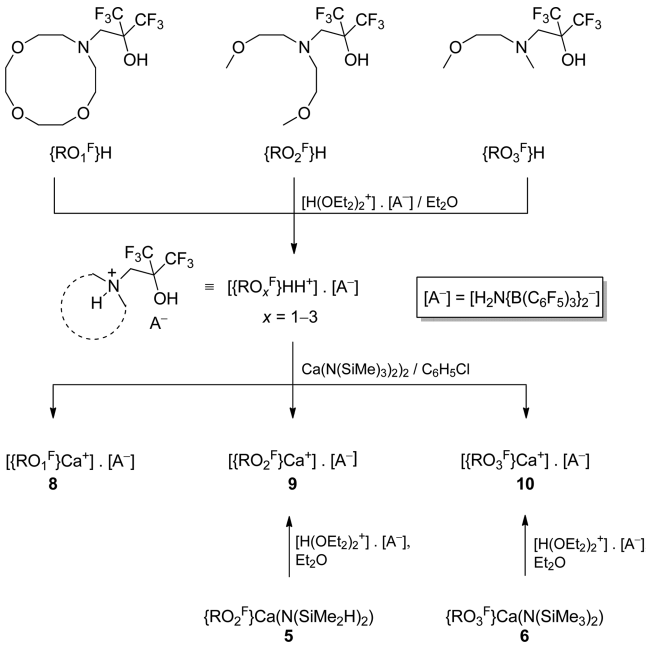

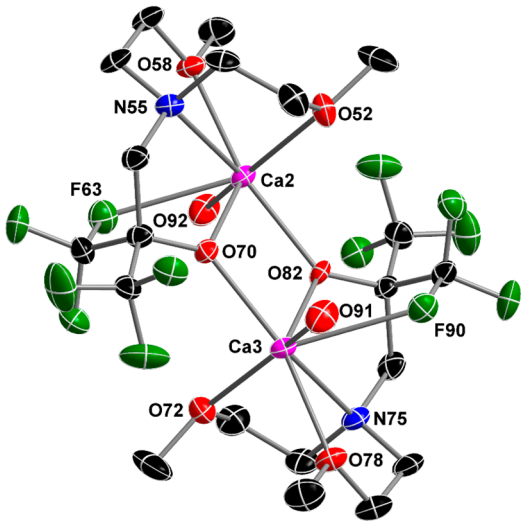

Figure 8. ORTEP representation of one of the two nonequivalent dimeric cations in the asymmetric unit of $[\{RO_2^F\}Ca^+(H_2O)]_2 \cdot 2[H_2N\{B(C_6F_5)_3\}_2^-]$ ($[\mathbf{9{\cdot}H_2O}]_2$), showing the coordinating H_2O molecules and Ca···F contacts. Counterions, hydrogen atoms, and noncoordinating solvent molecules are omitted for clarity. O(91) and O(92) correspond to the O atoms of coordinated water molecules. The Ca(2)···F(63) and Ca(3)···F(90) distances are in the range 2.70–2.75 Å.

and we found that they could only be dissolved in THF. ^{19}F and ^{11}B NMR in THF-d_8 testified to the integrity of the anion, but the existence of Ca···F interactions could not be probed by NMR spectroscopy owing to the mandatory use of this coordinating solvent. Attempts to grow single crystals of **8–10** suitable for X-ray diffraction studies were thwarted by their extreme sensitivity (electrophilicity) and affinity for water. Attempts using various crystallization techniques only afforded crystals of the water adducts $[\{RO_1^F\}Ca^+(H_2O)]_2 \cdot 2[H_2N\{B(C_6F_5)_3\}_2^-]$ ($[\mathbf{8{\cdot}H_2O}]_2$) and $[\{RO_2^F\}Ca^+(H_2O)]_2 \cdot 2[H_2N\{B(C_6F_5)_3\}_2^-]$ ($[\mathbf{9{\cdot}H_2O}]_2$), where the water molecules presumably came from the moisture background level.[34] Unsatisfactory refinement (final R1 = 9.52%) precludes precise discussion of the metric parameters in $[\mathbf{9{\cdot}H_2O}]_2$ (Figure 8), but several features can nonetheless be mentioned with confidence: (i) each asymmetric unit contains four anions and two structurally nonidentical dications of the general formula $[\{RO_2^F\}Ca^+(H_2O)]_2$, and Ca···F interactions (ca. 2.70–2.75 Å) are seen in only one of these, (ii) each of the four metal atoms is coordinated by a molecule of water, (iii) there is no contact between the cations and the anions, and (iv) unlike what is found in the charge-neutral parents, for each $\{RO_2^F\}$ ligand the coordination of *both* OCH_3 moieties onto the metal centers is seen. Evidently these observations point at the greater need for electron density in these cationic complexes, as highlighted by their ability to bind water from surrounding traces of moisture.

Even with the more chelating and electron-donating ligand $\{RO_1^F\}$, the Ca cations trapped residual water during the recrystallization of **8** in dichloromethane to afford the adduct $[\mathbf{8{\cdot}H_2O}]_2$. The structure of the dimeric cationic fragment depicted in Figure 9 shows the presence of a coordinated water molecule and a strong intramolecular Ca···F–C interaction (Ca(1)–F(21) = 2.650(3) Å; Ca(2)–F(67) = 2.651(3) Å) between each of the metal atoms and CF_3 groups of the ligand; there is no contact with the counterion. All attempts to grow water-free crystals of these species proved unsuccessful; note that under the same experimental conditions, the cationic $[\{RO_0^F\}Ca^+]_2 \cdot 2[H_2N\{B(C_6F_5)_3\}_2^-]$, where the ligand $\{RO_0^F\}^-$ contains one more $O_{heterocycle}$ atom than does $\{RO_0^F\}^-$ (see Chart 1), crystallized without binding water.[13]

Hydrophosphination Catalysis. Well-defined heteroleptic calcium complexes have emerged as potent precatalysts in atom-efficient hydroelementation reactions such as hydroamination and hydrophosphination of alkenes.[2] Yet, reports of calcium complexes in the hydrophosphination reactions of activated alkenes are confined to the use of precatalysts bearing bulky $\{^{Dipp}NacNac\}^-$,[7a] tridentate amidinate,[35] and iminoanilide ligands.[36] The fluorinated alkoxide calcium complexes **5–7** catalyze competently the addition of diphenylphosphine across the C=C vinylic bond in styrene under mild conditions (Table 4). Complex **4** was not included in this screening, as we found it was not sufficiently stable under catalysis conditions.

Characteristically for these calcium systems (and their heavier alkaline-earth congeners), this hydrophosphination reaction proceeds with strict 100% anti-Markovnikov regiose-

dx.doi.org/10.1021/om500343w | Organometallics 2014, 33, 5630–5642

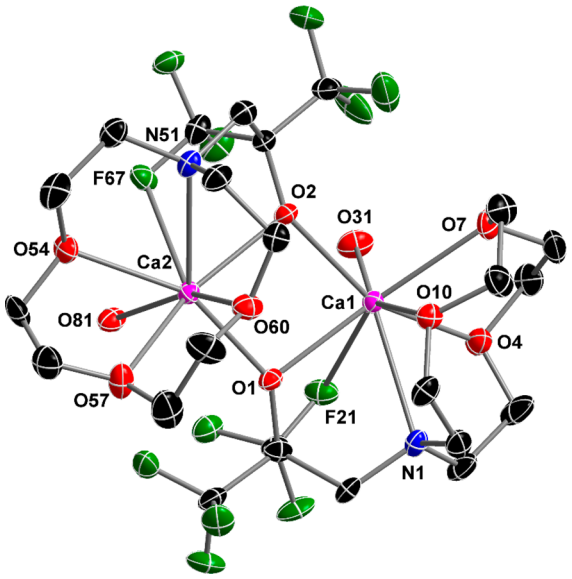

Figure 9. ORTEP representation of the dication in $[\{RO_1^F\}Ca^+(H_2O)]_2{\cdot}2[H_2N\{B(C_6F_5)_3\}_2^-]$ ($[\mathbf{8{\cdot}H_2O}]_2$), showing the coordinating H_2O molecules and Ca···F contacts. Counterions, hydrogen atoms, and noncoordinating solvent molecules are omitted for clarity. O(31) and O(81) are O atoms of coordinated water molecules.

lectivity at 60 °C. With as little as 1 mol % catalyst loading, the turnover numbers and frequencies observed with **5**–**7** for catalyzed reactions performed in the presence of solvent (entries 3–5) or with neat substrates (entries 6–11, apparent TOF ≈ 50 mol_{subst} mol_{Ca}^{-1} h^{-1}) compare well with those reported with other calcium-based precatalysts[7a,35,36] and place them among some of the most efficient systems reported to date for this challenging reaction.[35−37] Valuably, these complexes featured the same catalytic performances when higher substrate loadings were used (see e.g. entry 11). Under comparable conditions (entries 1–5), complexes **5**–**7** are generally more active than the simple bis(amido) complexes $Ca(N(SiMe_3)_2)_2(THF)_2$ and $Ca(N(SiMe_3)_2)_2$ (entries 1 and 2), showing the beneficial role of the fluorinated alkoxides.

Precatalysts with the $N(SiMe_2H)_2$ moiety perform somewhat better than those having a $N(SiMe_3)_2$ group. This observation, which is counterintuitive on the basis of pK_a considerations alone, is explained by the reduced stability of compounds **4** and **6** in solution (signs of decomposition of the metal complexes can be observed in a matter of hours under catalysis conditions), while on the other hand, complexes **5** and **7** are visually more stable (the first signs of decomposition occurring only after 24 h). This is tentatively attributed to the presence of Si−H moieties in **5** and **7**, which can impart stabilization to the metal through weak Ca···H−Si interactions. With zinc, the higher catalytic activity of cationic compounds with respect to their neutral analogues has been observed for the cyclohydroamination of aminoalkenes.[38] We found instead that **9** and **10** do not catalyze well the addition of $HPPh_2$ to styrene (entry 12), possibly because they are hampered by their limited solubility.

CONCLUSION

Potassium and heteroleptic calcium complexes supported by monoanionic fluorinated alkoxide ligands of varying denticity afford unusual coordination patterns in the solid state, forming polymetallic species which remain aggregated in solution. The calcium complexes **4**–**7** represent new additions to the small family of kinetically inert heteroleptic Ca mono(alkoxide) complexes, the most prominent example being Hanusa's $Ca(clox)(X)(THF)_x$ (clox = $OC(C_6H_5)_2CH_2C_6H_4$-Cl-4; X = I, x = 4; X = $N(SiMe_3)_2$, x = 3).[1c] Both potassium and calcium complexes are stabilized by a pattern of intramolecular M···F secondary interactions which contribute significantly to reach coordinative saturation around the metal atoms. In addition, although definitive evidence for agostic Ca···H−Si interactions could not be found, it is undeniable that the $[Ca]-N(SiMe_2H)_2$ complexes **5** and **7** are less labile than their $[Ca]-N(SiMe_3)_2$ derivatives **4** and **6**. The heteroleptic complexes **4**–**7** can serve as synthetic precursors to solvent-free discrete cationic Ca complexes which exhibit extreme

Table 4. Hydrophosphination of Styrene with Ph_2PH Catalyzed by the Calcium Amide Compounds 5–7 and Cationic Complex 10

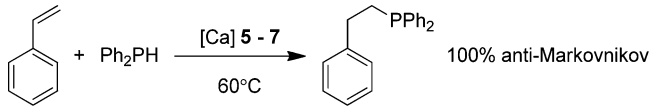

entry	catalyst	$[styrene]_0:[HPPh_2]_0:[Ca]_0$	t (h)	conversion[a] (%)	TOF (mol_{subst} mol_{Ca}^{-1} h^{-1})
1[b]	$Ca(N(SiMe_3)_2)_2(THF)_2$	50:50:1	24	53	1.1
2[b]	$Ca(N(SiMe_3)_2)_2$	50:50:1	24	55	1.3
3[b]	$\{RO_2^F\}Ca(N(SiMe_2H)_2)$ (**5**)	50:50:1	24	85	1.8
4[b]	$\{RO_3^F\}Ca(N(SiMe_3)_2)$ (**6**)	50:50:1	24	46	1.0
5[b]	$\{RO_3^F\}Ca(N(SiMe_2H)_2)$ (**7**)	50:50:1	24	69	1.4
6[c]	$\{RO_2^F\}Ca(N(SiMe_2H)_2)$ (**5**)	50:50:1	1	99	50
7[c]	$\{RO_3^F\}Ca(N(SiMe_3)_2)$ (**6**)	50:50:1	1	87	44
8[c]	$\{RO_3^F\}Ca(N(SiMe_3)_2)$ (**6**)	100:100:1	2	99	45
9[c]	$\{RO_3^F\}Ca(N(SiMe_2H)_2)$ (**7**)	50:50:1	1	82	41
10[c]	$\{RO_3^F\}Ca(N(SiMe_2H)_2)$ (**7**)	100:100:1	2	99	45
11[c]	$\{RO_3^F\}Ca(N(SiMe_2H)_2)$ (**7**)	400:400:1	2	26	52
12[c]	$\{RO_3^F\}Ca^+{\cdot}A^-$ (**10**)	50:50:1	2	8	2.0

[a]Conversion determined by ^1H NMR spectroscopy. [b]Conditions: 10 μmol of precatalyst, [Ca] = 16.67 mM, 0.6 mL of C_6D_6, 60 °C. [c]Conditions: 10 μmol of precatalyst, no solvent, 60 °C.

dx.doi.org/10.1021/om500343w | Organometallics 2014, 33, 5630−5642

electrophilicity and capture even traces of residual water molecules. They also act as potent precatalysts for the 100% anti-Markovnikov hydroelementation of styrene with diphenylphosphine, displaying activities in the upper range of those reported for this reaction. Following these encouraging results, we are now aiming at exploiting these new Ca mono(alkoxide) complexes for the catalysis of a variety of atom-efficient organic transformations.

EXPERIMENTAL SECTION

General Procedures. All manipulations were performed under an inert atmosphere using standard Schlenk techniques or in a dry, solvent-free glovebox (Jacomex; O_2 <1 ppm, H_2O <5 ppm) for catalyst loading. CaI_2 (Aldrich, 99.999 anhydrous beads %) and $HPPh_2$ were used as received. $HN(SiMe_3)_2$ (Acros) and $HN(SiMe_2H)_2$ were dried over CaH_2 and distilled prior to use. Styrene was dried and distilled over CaH_2 and stored over 3 Å molecular sieves. The compounds $[H(OEt_2)_2^+]\cdot[H_2N\{(B(C_6F_5)_3\}_2^-]$,[31] $Ca(N(SiMe_3)_2)_2$,[39] $Ca(N(SiMe_3)_2)_2(THF)_2$,[40] and $Ca(N(SiMe_2H)_2)_2(THF)$[9] were prepared following literature protocols. Solvents (THF, Et_2O, CH_2Cl_2, pentane, and toluene) were purified and dried (water contents all below 10 ppm) over alumina columns (MBraun SPS). THF was further distilled under argon from sodium mirror/benzophenone ketyl prior to use. All deuterated solvents (Eurisotop, Saclay, France) were stored in sealed ampules over activated 3 Å molecular sieves and were thoroughly degassed by several freeze−thaw−vacuum cycles.

NMR spectra were recorded on Bruker AM-400 and AM-500 spectrometers. All ^1H and $^{13}C\{^1H\}$ chemical shifts were determined using residual signals of the deuterated solvents and were calibrated vs $SiMe_4$. $^{29}Si\{^1H\}$ chemical shifts were determined against $Si(SiMe_3)_4$. Assignment of the signals was carried out using 1D (^1H, $^{13}C\{^1H\}$) and 2D (COSY, HMBC, HMQC) NMR experiments. Coupling constants are given in hertz. $^{19}F\{^1H\}$ chemical shifts were determined by external reference to an aqueous solution of $NaBF_4$. PGSE NMR experiments were carried out on a Bruker Avance III 400 MHz spectrometer equipped with a BBOF pulsed field-gradient probe using a bipolar gradient pulse stimulated echo sequence. Each experiment was performed on a 0.1 M solution at 298 K using a spectral width of 4807 Hz, a 90° pulse width of 11.5 μs, a diffusion delay time of 0.05 s, and a total diffusion-encoding pulse width of 0.0016 s. The diffusion encoding pulse strength was arrayed from 0 to 35 G cm^{-2} over 12 or 16 increments with 4 dummy scans and 8 scans per increment. The method used to determine hydrodynamic radii was identical with that reported elsewhere.[24]

Elemental analyses were performed on a Carlo Erba 1108 Elemental Analyzer instrument at the London Metropolitan University by Stephen Boyer and were the average of a minimum of two independent measurements.

$\{RO_1^F\}H$. A solution of 1-aza-12-crown-4 (0.49 g, 2.81 mmol) in Et_2O (5 mL) was added dropwise at 0 °C to a solution of 2,2-bis(trifluoromethyl)oxirane (0.55 g, 3.05 mmol) in Et_2O (5 mL). The reaction mixture was warmed to room temperature and stirred for 2 days. The volatiles were then evaporated under reduced pressure to afford $\{RO_1^F\}H$ as a colorless solid (0.88 g, 88%). X-ray-quality crystals were obtained by slow concentration of a solution of the title compound in Et_2O. ^1H NMR (C_6D_6, 500.13 MHz, 25 °C): δ 6.80 (s, 1H, O*H*), 3.34−3.30 (m, 4H, OCH_2 moieties), 3.29−3.25 (m, 4H, OCH_2 moieties), 3.24−3.20 (m, 4H, OCH_2 moieties), 2.79 (s, 2H, CH_2C$(CF_3)_2$), 2.41−2.31 (m, 4H, NCH_2CH_2) ppm. $^{13}C\{^1H\}$ NMR (C_6D_6, 125.75 MHz, 25 °C): δ 124.61 (q, $^1J_{CF}$ = 288.2 Hz, CF_3), 73.97 (hept, $^2J_{CF}$ = 28.3 Hz, $C(CF_3)_2$), 70.60, 70.39, 69.05 (all OCH_2 moieties), 57.85 (CH_2C$(CF_3)_2$), 55.68 (NCH_2CH_2) ppm. $^{19}F\{^1H\}$ NMR (C_6D_6, 376.52 MHz, 25 °C): δ −77.21 (s, 6F, CF_3) ppm. Anal. Calcd for $C_{12}H_{19}F_6NO_4$ (355.27): C, 40.5; H, 5.4; N, 3.9. Found: C, 40.7; H, 5.3; N, 4.0. Mass spectrometry ESI: $[M + Na^+]$ ($C_{12}H_{19}F_6NO_4Na$) calcd m/z 378.1116, found 378.1112.

The protio ligands $\{RO_2^F\}H$ and $\{RO_3^F\}H$ were prepared in the same way (Supporting Information).

$\{RO_1^F\}K$ (1). $KN(SiMe_3)_2$ (56 mg, 0.56 mmol) was added in portions with a bent glass finger to a solution of $\{RO_1^F\}H$ (100 mg, 0.56 mmol) in Et_2O (10 mL). A white precipitate formed immediately. The reaction mixture was stirred overnight at room temperature. The volatiles were removed in vacuo, and the resulting solid was washed with pentane (4 × 5 mL) to yield **1** as a colorless solid (88 mg, 80%). The product displayed poor solubility in hydrocarbon and ether solvents and was soluble only in CH_2Cl_2. X-ray-quality crystals were obtained by recrystallization from a concentrated CD_2Cl_2 solution at room temperature. ^1H NMR (CD_2Cl_2, 500.13 MHz, 25 °C): δ 3.73−3.51 (m, 12H, all crown ether), 2.71 (overlapping m, 6H, NCH_2CH_2 and CH_2C$(CF_3)_2$) ppm. $^{13}C\{^1H\}$ NMR (CD_2Cl_2, 125.75 MHz, 25 °C): δ 127.81 (q, $^1J_{CF}$ = 298.2 Hz, CF_3), 67.14, 66.63, 66.25 (all crown ether), 59.88 (CH_2C$(CF_3)_2$), 54.80 (NCH_2CH_2) ppm; the resonance for $C(CF_3)_2$) could not be detected. $^{19}F\{^1H\}$ NMR (CD_2Cl_2, 376.52 MHz, 25 °C): δ −78.41 (s, 6F, CF_3) ppm. Anal. Calcd for $C_{12}H_{18}F_6KNO_4$ (393.36): C, 36.6; H, 4.6; N, 3.6. Found: C, 36.6; H, 3.8; N, 3.8.

$\{RO_2^F\}K$ (2). $KN(SiMe_2H)_2$ (0.10 g, 0.59 mmol) was added in portions with a bent glass finger to a solution of $\{RO_2^F\}H$ (0.18 g, 0.59 mmol) in Et_2O (5 mL). The reaction mixture was stirred overnight at room temperature. The volatiles were removed in vacuo to give a colorless solid. Extraction with pentane (20 mL) and evaporation of the volatiles afforded **2** as a colorless solid (0.16 g, 78%). X-ray-quality crystals were obtained by recrystallization from a concentrated pentane solution. ^1H NMR (C_6D_6, 300.13 MHz, 25 °C): δ 3.23 (t, 4H, $^3J_{HH}$ = 5.1 Hz, CH_2OCH_3), 3.07 (s, 6H, OCH_3), 3.00 (s, 2H, CH_2C$(CF_3)_2$), 2.78 (t, 4H, $^3J_{HH}$ = 5.1 Hz, NCH_2CH_2) ppm. $^{13}C\{^1H\}$ NMR (75.46 MHz, C_6D_6, 25 °C): δ 127.61 (q, $^1J_{CF}$ = 297.2 Hz, CF_3), 82.43 (hept, $^2J_{CF}$ = 22.8 Hz, $C(CF_3)_2$), 69.20 (CH_2OCH_3), 58.19 (OCH_3), 57.92 (NCH_2CH_2), 53.77 (CH_2C$(CF_3)_2$) ppm. $^{19}F\{^1H\}$ NMR (C_6D_6, 376.52 MHz, 25 °C): δ −77.17 (s, 6F, CF_3) ppm. Anal. Calcd for $C_{10}H_{16}F_6KNO_3$ (351.33): C, 34.2; H, 4.6; N, 4.0. Found: C, 34.3; H, 4.7; N, 4.1.

$\{RO_3^F\}K$ (3). $KN(SiMe_2H)_2$ (0.55 g, 3.20 mmol) was added in portions with a bent glass finger to a solution of $\{RO_3^F\}H$ (0.90 g, 3.34 mmol) in Et_2O (30 mL). The reaction mixture was stirred overnight at room temperature. The volatiles were removed in vacuo to yield **3** as a colorless solid (0.95 g, 93%). X-ray-quality crystals were obtained by recrystallization from a concentrated pentane solution at room temperature. ^1H NMR (C_6D_6, 400.13 MHz, 25 °C): δ 3.03 (s, 3H, OCH_3), 2.92 (t, 2H, $^3J_{HH}$ = 4.6 Hz, CH_2OCH_3), 2.75 (s, 2H, CH_2C$(CF_3)_2$), 2.32 (br, 2H, NCH_2), 2.17 (s, 3H, NCH_3) ppm. $^{13}C\{^1H\}$ NMR (100.62 MHz, C_6D_6, 25 °C): δ 126.46 (q, $^1J_{CF}$ = 296.1 Hz, CF_3), 82.86 (hept, $^2J_{CF}$ = 23.1 Hz, $C(CF_3)_2$), 69.76 (OCH_3), 62.28 (CH_2OCH_3), 59.74 (CH_2C$(CF_3)_2$), 58.25 (NCH_2CH_2), 43.15 (NCH_3) ppm. $^{19}F\{^1H\}$ NMR (C_6D_6, 376.52 MHz, 25 °C): δ −77.30 (s, 6F, CF_3) ppm. Anal. Calcd for $C_8H_{12}F_6KNO_2$ (307.28): C, 31.3; H, 3.9; N, 4.6. Found: C, 31.2; H, 3.1; N, 3.9.

$\{RO_2^F\}Ca(N(SiMe_3)_2)$ (4). A solution of $\{RO_2^F\}H$ (0.23 g, 0.73 mmol) in pentane (10 mL) was added at −78 °C over a period of 1 h to a solution of $Ca(N(SiMe_3)_2)_2(THF)_2$ (0.44 g, 0.88 mmol) in pentane (10 mL). The mixture was warmed to room temperature and stirred overnight, and the volatiles were removed under vacuum. The resulting powder was stripped with pentane (3 × 4 mL) and dried in vacuo to give a brown powder, which was dissolved in toluene (5 mL). Layering of the resulting solution with pentane (15 mL) resulted in the formation of a brown oil. The oil was removed by filtration, and the remaining solution was stored in a freezer at −28 °C to afford **5** as colorless crystals (50 mg, 13%; not optimized). ^1H NMR (THF-d_8, 500.13 MHz, 25 °C): δ 3.70 (t, $^3J_{HH}$ = 5.3 Hz, 4H, NCH$_2$CH_2), 3.63 (s, 6H, OCH_3), 2.85−2.80 (overlapping m, 6H, NCH_2CH_2 and CH_2C$(CF_3)_2$), −0.05 (s, 18H, NSi(CH_3)$_3$) ppm. $^{13}C\{^1H\}$ NMR (THF-d_8, 125.73 MHz, 25 °C): δ 127.24 (q, CF_3, $^1J_{CF}$ = 292.0 Hz), 82.33 (hept, $C(CF_3)_2$, $^2J_{CF}$ = 25.9 Hz), 70.31 (NCH$_2$CH$_2$), 61.16 (OCH$_3$), 56.23 (CH$_2$C$(CF_3)_2$), 53.68 (NCH$_2$CH$_2$), 5.92 (NSi(CH$_3$)$_3$) ppm. $^{19}F\{^1H\}$ NMR (THF-d_8, 376.45 MHz, 25 °C): δ −81.78 (s, 6F, CF_3) ppm. Anal. Calcd for $C_{16}H_{34}CaF_6N_2O_3Si_2$ (512.69): C, 37.5; H, 6.7; N, 5.5. Found: C, 37.6; H, 6.5; N, 5.6.

dx.doi.org/10.1021/om500343w | Organometallics 2014, 33, 5630−5642

{RO$_2^F$}Ca(N(SiMe$_2$H)$_2$) (5). A solution of {RO$_2^F$}H (0.18 g, 0.57 mmol) in Et$_2$O (10 mL) was added at −78 °C over a period of 1 h to a solution of Ca(N(SiMe$_2$H)$_2$)$_2$(THF) (0.28 g, 0.76 mmol) in Et$_2$O (10 mL). The mixture was warmed to room temperature and stirred overnight, and the volatiles were removed under vacuum. The resulting powder was stripped with pentane (3 × 4 mL) and dried in vacuo to give analytically pure **3** as an off-white powder (0.22 g, 79%). Single crystals of **5** suitable for X-ray diffraction crystallography were obtained by recrystallization from Et$_2$O at room temperature. ^{1}H NMR (C$_6$D$_6$, 400.13 MHz, 25 °C): δ 4.88 (m, 2H, $^1J_{SiH}$ = 162 Hz, Si*H*), 3.22−3.14 (m, 2H, C*H*$_2$OCH$_3$), 3.03−2.89 (overlapping m, 12H, *CH*$_2$OCH$_3$, *CH*$_2$C(CF$_3$)$_2$ and NC*H*$_2$CH$_2$), 2.47 (d, 2H, $^2J_{HH}$ = 12.4 Hz, NC*H*(H)), 0.47 (d, 12H, $^3J_{HH}$ = 2.5 Hz, Si(*CH*$_3$)$_2$H) ppm. ^{13}C{^{1}H}NMR (100.62 MHz, C$_6$D$_6$, 25 °C): δ 125.84 (q, $^1J_{CF}$ = 290.1 Hz, *CF*$_3$), 79.30 (hept, $^2J_{CF}$ = 25.7 Hz, *C*(CF$_3$)$_2$), 69.35 (*CH*$_2$OCH$_3$), 59.46 (OCH$_3$), 55.45 (*CH*$_2$C(CF$_3$)$_2$), 53.45 (NCH$_2$CH$_2$), 5.02 (Si(*CH*$_3$)$_2$H) ppm. ^{19}F{^{1}H} NMR (376.52 MHz, C$_6$D$_6$, 25 °C): δ −77.64 (s, 6F, *CF*$_3$) ppm. ^{29}Si{^{1}H} NMR (C$_6$D$_6$, 79.49 MHz, 25 °C): δ −25.1 ppm. FTIR (Nujol in KBr plates): $\tilde{\nu}_{Si-H}$ 2016 (s) cm^{-1}. Anal. Calcd for C$_{14}$H$_{30}$CaF$_6$N$_2$O$_3$Si$_2$ (484.64): C, 34.7; H, 6.2; N, 5.8. Found: C, 34.4; H, 6.4; N, 5.7.

{RO$_3^F$}Ca(N(SiMe$_3$)$_2$) (6). A solution of {RO$_3^F$}H (0.34 g, 1.26 mmol) in Et$_2$O (15 mL) was added at −78 °C over a period of 1 h to a solution of Ca(N(SiMe$_3$)$_2$)$_2$ (0.45 g, 1.26 mmol) in Et$_2$O (20 mL). The reaction mixture was warmed to room temperature and stirred overnight, and the volatiles were removed under vacuum. The resulting powder was stripped with pentane (3 × 4 mL) and dried in vacuo to give **6** as a yellow powder (0.42 g, 71%). Single crystals of **2** suitable for X-ray diffraction crystallography were obtained by recrystallization from C$_6$D$_6$. ^{1}H NMR (C$_6$D$_6$, 500.13 MHz, 25 °C): δ 3.03 (overlapping m, 5H, OC*H*$_3$ and C*H*$_2$OCH$_3$), 2.39 (ABq, 2H, $\Delta\delta_{AB}$ = 0.08, J_{AB} = 14.8 Hz, *CH*$_2$C(CF$_3$)$_2$), 2.12 (s, 3H, NC*H*$_3$), 2.02 (m, 2H, NC*H*$_2$CH$_2$), 0.35 (s, 18H, NSi(*CH*$_3$)$_3$) ppm. ^{13}C{^{1}H} NMR (C$_6$D$_6$, 125.75 MHz, 25 °C): δ 125.70 (q, $^1J_{CF}$ = 290.8 Hz, C(*CF*$_3$)$_2$), 125.46 (q, $^1J_{CF}$ = 289.6 Hz, *CF*$_3$), 79.66 (hept, $^2J_{CF}$ = 25.3 Hz, *C*(CF$_3$)$_2$), 69.53 (*CH*$_2$OCH$_3$), 60.90 (OCH$_3$), 59.75 (NCH$_2$CH$_2$), 58.43 (*CH*$_2$C(CF$_3$)$_2$), 45.70 (NCH$_3$), 6.43 (Si(*CH*$_3$)$_3$) ppm. ^{19}F{^{1}H} NMR (C$_6$D$_6$, 376.52 MHz, 25 °C): δ −73.39 (q, 3F, $^4J_{FF}$ = 9.4 Hz, *CF*$_3$), −75.14 (q, 3F, $^4J_{FF}$ = 9.4 Hz, *CF*$_3$) ppm. ^{29}Si{^{1}H} NMR (C$_6$D$_6$, 79.49 MHz, 25 °C): δ −14.3 ppm. Satisfactory elemental analysis for C$_{14}$H$_{30}$CaF$_6$N$_2$O$_2$Si$_2$ (468.64; C, 35.9; H, 6.5; N, 6.0) could not be obtained in spite of repeated attempts.

{RO$_3^F$}Ca(N(SiMe$_2$H)$_2$) (7). A solution of {RO$_3^F$}H (0.15 g, 0.55 mmol) in Et$_2$O (10 mL) was added at −78 °C over a period of 1 h to a solution of Ca(N(SiMe$_2$H)$_2$)(THF) (0.28 g, 0.74 mmol) in Et$_2$O (10 mL). The reaction mixture was warmed to room temperature and stirred overnight, and the volatiles were removed under vacuum. The resulting powder was stripped with pentane (3 × 4 mL) and dried in vacuo to give pure **4** as an off-white powder (0.18 g, 73%). Single crystals of 7 suitable for X-ray diffraction crystallography were obtained by recrystallization from Et$_2$O at room temperature. ^{1}H NMR (C$_6$D$_6$, 400.13 MHz, 25 °C): δ 4.86 (m, 2H, $^1J_{SiH}$ = 162 Hz, Si*H*), 3.12 (s, 3H, OC*H*$_3$), 2.84−2.61 (overlapping m, 4H, C*H*$_2$OCH$_3$ and NC*H*$_2$CH$_2$), 2.51 (ABq, 2H, $\Delta\delta_{AB}$ = 0.12, $^2J_{AB}$ = 15.1 Hz, *CH*$_2$C(CF$_3$)$_2$), 2.03 (s, 3H, NC*H*$_3$), 0.45 (d, 12H, J = 2.5 Hz, Si(*CH*$_3$)$_2$H) ppm. ^{13}C{^{1}H} NMR (C$_6$D$_6$, 100.62 MHz, 25 °C): δ 125.92 (q, $^1J_{CF}$ = 289.9 Hz, *CF*$_3$), 125.36 (q, $^1J_{CF}$ = 290.1 Hz, *CF*$_3$), 79.45 (hept, $^2J_{CF}$ = 25.8 Hz, *C*(CF$_3$)$_2$), 69.39 (*CH*$_2$OCH$_3$), 60.15 (OCH$_3$), 59.26 (*CH*$_2$C(CF$_3$)$_2$), 58.60 (NCH$_2$CH$_2$), 43.28 (NCH$_3$), 5.09 (Si(*CH*$_3$)$_2$H), 4.82 (Si(CH$_3$)$_2$H) ppm. ^{19}F{^{1}H} NMR (C$_6$D$_6$, 376.52 MHz, 25 °C): δ −76.48 (q, 3F, $^4J_{FF}$ = 9.2 Hz, *CF*$_3$), −76.81 (q, 3F, $^4J_{FF}$ = 9.3 Hz, *CF*$_3$) ppm. ^{29}Si{^{1}H} NMR (C$_6$D$_6$, 79.49 MHz, 25 °C): δ −25.4 ppm. FTIR (Nujol in KBr plates): $\tilde{\nu}_{Si-H}$ 2015 (s) cm^{-1}. Anal. Calcd for C$_{12}$H$_{26}$CaF$_6$N$_2$O$_2$Si$_2$ (440.59): C, 32.7; H, 6.0; N, 6.4. Found: C, 32.3; H, 6.0; N, 6.2.

[{RO$_1^F$}Ca$^+$]·[H$_2$N{B(C$_6$F$_5$)$_3$}$_2^-$] (8). [{RO$_1^F$}HH$^+$]·[H$_2$N{(B(C$_6$F$_5$)$_3$}$_2$]$^-$ (132 mg, 0.09 mmol) was added in portions with a bent glass finger to a solution of Ca(N(SiMe$_3$)$_2$)$_2$ (34 mg, 0.09 mmol) in C$_6$H$_5$Cl (5 mL). Stirring was continued at room temperature for 2 days. The solution was evaporated in vacuo, and the resulting colorless solid was purified by reprecipitation from CH$_2$Cl$_2$ with pentane (three times). The final colorless powder was dried in vacuo to afford analytically pure **8** (96 mg, 70%). ^{1}H NMR (THF-d_8, 400.13 MHz, 25 °C): δ 5.74 (br, 2H, N*H*$_2$), 4.06−3.93 (m, 8H, OC*H*$_2$ moieties), 3.93−3.82 (m, 4H, OC*H*$_2$ moieties), 3.12−2.75 (overlapping m, 6H, NC*H*$_2$CH$_2$ and C*H*$_2$C(CF$_3$)$_2$) ppm. ^{13}C{^{1}H} NMR (THF-d_8, 100.62 MHz, 25 °C): δ 150.08, 147.69, 141.39, 138.85, 136.36 (all C$_6$F$_5$), 126.99 (q, $^1J_{CF}$ = 292.8 Hz, CF$_3$), 72.36, 71.16, 70.75 (all OCH$_2$ moieties), 59.51 (CH$_2$C(CF$_3$)$_2$), 54.01 (NCH$_2$CH$_2$) ppm; the resonance for *C*(CF$_3$)$_2$) was not observed. ^{19}F NMR (THF-d_8, 376.52 MHz, 25 °C): δ −79.49 (s, 6F, *CF*$_3$), −133.13 (d, 12F, $^3J_{FF}$ = 18.4 Hz, *o*-F), −161.14 (t, 6F, $^3J_{FF}$ = 20.2 Hz, *p*-F), −166.44 (t, 12F, $^3J_{FF}$ = 19.3 Hz, *m*-F) ppm. ^{11}B NMR (THF-d_8, 128.38 MHz, 25 °C): δ −8.31 ppm. Anal. Calcd for C$_{48}$H$_{20}$B$_2$CaF$_{36}$N$_2$O$_4$ (1434.33): C, 40.2; H, 1.4; N, 2.0. Found: C, 40.1; H, 1.3; N, 2.1.

[{RO$_2^F$}Ca$^+$]·[H$_2$N{B(C$_6$F$_5$)$_3$}$_2^-$] (9). *Method A.* [{RO$_2^F$}HH$^+$]·[H$_2$N{(B(C$_6$F$_5$)$_3$}$_2^-$] (0.15 g, 0.11 mmol) was added in portions with a bent glass finger to a solution of Ca(N(SiMe$_3$)$_2$)$_2$ (37 mg, 0.11 mmol) in C$_6$H$_5$Cl (10 mL). The stirring was continued at room temperature for 2 days. The solution was evaporated under dynamic vacuum, and the resulting colorless solid was purified by repeated reprecipitation from CH$_2$Cl$_2$ with pentane (three times). Drying under vacuum to constant weight afforded **9** as a colorless powder (97 mg, 63%).

Method B. [H(OEt$_2$)$_2^+$]·[H$_2$N{(B(C$_6$F$_5$)$_3$}$_2^-$] (97 mg, 0.08 mmol) was added in portions to a solution of **5** (40 mg, 0.08 mmol) in Et$_2$O (10 mL). A colorless precipitate formed after a few minutes. The stirring was continued overnight at room temperature. The solution was then filtered to isolate a solid, which was purified by repeated reprecipitation from CH$_2$Cl$_2$ with pentane (three times). The title compound was isolated as a colorless powder after drying in vacuo (85 mg, 75%). ^{1}H NMR (THF-d_8, 500.13 MHz, 25 °C): δ 5.74 (br, 2H, N*H*$_2$), 3.78 (t, 4H, $^3J_{HH}$ = 4.8 Hz, C*H*$_2$OCH$_3$), 3.49 (s, 6H, OC*H*$_3$), 2.94 (s, 2H, *CH*$_2$C(CF$_3$)$_2$), 2.90 (t, 4H, $^3J_{HH}$ = 5.1 Hz, NC*H*$_2$CH$_2$) ppm. ^{13}C{^{1}H} NMR (THF-d_8, 125.75 MHz, 25 °C): δ 149.90, 148.01, 141.18, 139.23, 138.64, 136.70 (all C$_6$F$_5$), 127.06 (q, $^1J_{CF}$ = 292.0 Hz, CF$_3$), 70.87 (*CH*$_2$OCH$_3$), 60.26 (OCH$_3$), 56.89 (*CH*$_2$C(CF$_3$)$_2$), 54.41 (NCH$_2$CH$_2$) ppm; the resonance for *C*(CF$_3$)$_2$) was not observed. ^{19}F NMR (THF-d_8, 376.52 MHz, 25 °C): δ −79.68 (s, 6F, *CF*$_3$), −133.13 (d, 12F, $^3J_{FF}$ = 18.4 Hz, *o*-F), −161.14 (t, 6F, $^3J_{FF}$ = 20.2 Hz, *p*-F), −166.44 (t, 12F, $^3J_{FF}$ = 19.3 Hz, *m*-F) ppm. ^{11}B NMR (THF-d_8, 128.38 MHz, 25 °C): δ −8.35 ppm. Anal. Calcd for C$_{46}$H$_{18}$B$_2$CaF$_{36}$N$_2$O$_3$ (1392.29): C, 39.7; H, 1.3; N, 2.0. Found: C, 39.6; H, 1.3; N, 2.1.

[{RO$_3^F$}Ca$^+$]·[H$_2$N{B(C$_6$F$_5$)$_3$}$_2^-$] (10). *Method A.* [{RO$_3^F$}HH$^+$]·[H$_2$N{(B(C$_6$F$_5$)$_3$}$_2^-$] (200 mg, 0.15 mmol) was added in portions to a solution of Ca(N(SiMe$_3$)$_2$)$_2$ (54 mg, 0.15 mmol) in C$_6$H$_5$Cl (5 mL). The stirring was continued at room temperature for 2 days. The volatile fraction was evaporated under vacuum to give a solid which was purified by repeated reprecipitation from CH$_2$Cl$_2$ with pentane (three times). The colorless powder was dried in vacuo to afford analytically pure **10** (164 mg, 80%).

Method B. [H(OEt$_2$)$_2^+$]·[H$_2$N{(B(C$_6$F$_5$)$_3$}$_2^-$] (76 mg, 0.06 mmol) was added in portions to a solution of **6** (30 mg, 0.06 mmol) in Et$_2$O (10 mL). A colorless precipitate formed within a few minutes. Stirring was continued overnight at room temperature. The solution was filtered out, and the colorless solid was purified by repeated reprecipitation from CH$_2$Cl$_2$ with pentane (three times). The crude sample contained residual Et$_2$O, which could not be removed. The powder was dried in vacuo to afford **10** (66 mg, 76%) as a colorless powder. ^{1}H NMR (THF-d_8, 400.13 MHz, 25 °C): δ 5.74 (br, 2H, N*H*$_2$), 3.78 (t, 2H, $^3J_{HH}$ = 5.2 Hz, C*H*$_2$OCH$_3$), 3.55 (s, 3H, OC*H*$_3$), 2.90−2.70 (overlapping m, 4H, NC*H*$_2$CH$_2$ and C*H*$_2$C(CF$_3$)$_2$), 2.38 (s, 3H, NC*H*$_3$) ppm. ^{13}C{^{1}H} NMR (THF-d_8, 100.62 MHz, 25 °C): δ 150.08, 147.71, 141.40, 138.87, 136.39 (all C$_6$F$_5$), 126.88 (q, $^1J_{CF}$ = 293.8 Hz, CF$_3$), 71.53 (*CH*$_2$OCH$_3$), 61.21 (OCH$_3$), 60.01 (CH$_2$C(CF$_3$)$_2$), 58.92 (NCH$_2$CH$_2$), 43.66 (NCH$_3$) ppm; the resonance for *C*(CF$_3$)$_2$) was not observed. ^{19}F NMR (THF-d_8, 376.52 MHz, 25 °C): δ −79.16 (s, *CF*$_3$), −133.13 (d, $^3J_{FF}$ = 17.7 Hz, 12F, *o*-F), −161.15 (t, $^3J_{FF}$ = 20.2 Hz, 6F, *p*-F), −166.45 (t, $^3J_{FF}$ = 19.0 Hz, 12 F, *m*-F) ppm.

dx.doi.org/10.1021/om500343w | *Organometallics* 2014, 33, 5630−5642

^{11}B NMR (THF-d_8, 128.38 MHz, 25 °C): δ −10.21 ppm. Anal. Calcd for $C_{44}H_{14}B_2CaF_{36}N_2O_2$ (1348.24): C, 39.2; H, 1.0; N, 2.1. Found: C, 39.2; H, 1.1; N, 2.2.

Typical Procedure for Hydrophosphination Reactions. In the glovebox, the precatalyst was loaded in an NMR tube. All subsequent operations were carried out on a vacuum manifold using Schlenk techniques. The required amount of solvent was added with a syringe to the precatalyst, followed by addition of styrene and $HPPh_2$. The NMR tube was immerged in an oil bath set at the desired temperature, and the reaction time was measured from this point. The reaction was terminated by addition of "wet" C_6D_6 to the reaction mixture.

■ ASSOCIATED CONTENT

Supporting Information

Text, figures, tables, and CIF files giving details of the synthesis and characterization of $\{RO_0^F\}K$, $\{RO_x^F\}H$, and $[\{RO_x^F\}HH^+]\cdot[H_2N\{B(C_6F_5)_3\}_2^-]$, X-ray structures of $\{RO_0^F\}K$, $\{RO_1^F\}H$, and $[\{RO_x^F\}HH^+]\cdot[H_2N\{B(C_6F_5)_3\}_2^-]$, crystallographic data for **1**−**3**, $[\mathbf{4}]_2$−$[\mathbf{7}]_2$, $[\mathbf{8}\cdot\mathbf{H_2O}]_2$, $[\mathbf{9}\cdot\mathbf{H_2O}]_2$, and bond valence analysis. This material is available free of charge via the Internet at http://pubs.acs.org.

■ AUTHOR INFORMATION

Corresponding Authors

*E-mail for J.-F.C.: jean-francois.carpentier@univ-rennes1.fr.

*E-mail for Y.S.: yann.sarazin@univ-rennes1.

Notes

The authors declare no competing financial interest.

■ ACKNOWLEDGMENTS

The authors thank the *Agence Nationale de la Recherche* for financial support (Ph.D. grant to S.-C.R., ANR-11-BS07-009-01 GreenLAkE). Assistance from J.-P. Guégan (PGSE NMR, ISC Rennes) and S. Boyer (elemental analysis, London Metropolitan University) is most appreciated.

■ REFERENCES

(1) See for instance: (a) Williams, R. A.; Hanusa, T. P.; Huffman, J. C. *Organometallics* **1990**, *9*, 1128. (b) Hanusa, T. P. *Polyhedron* **1990**, *9*, 1345 (review article). (c) Williams, R. A.; Tesh, K. F.; Hanusa, T. P. *J. Am. Chem. Soc.* **1991**, *113*, 4843. (d) Harvey, M. J.; Hanusa, T. P.; Young, V. G., Jr. *Angew. Chem., Int. Ed.* **1999**, *38*, 217. (e) Hanusa, T. P. *Coord. Chem. Rev.* **2000**, *210*, 329.

(2) (a) Harder, S. *Chem. Rev.* **2010**, *110*, 3852. (b) Barrett, A. G. M.; Crimmin, M. R.; Hill, M. S.; Procopiou, P. A. *Proc. R. Soc. A* **2010**, *466*, 927. (c) *Topics in Organometallic Chemistry*; Harder, S., Vol. Ed.; Springer: Berlin, 2013; Vol. *45*.

(3) See for instance: (a) Westerhausen, M. *Inorg. Chem.* **1991**, *30*, 96. (b) Westerhausen, M. *Angew. Chem., Int. Ed.* **2001**, *40*, 2975. (c) Fischer, R.; Gaertner, M.; Goerls, H.; Westerhausen, M. *Angew. Chem., Int. Ed.* **2006**, *45*, 609. (d) Westerhausen, M.; Gaertner, M.; Fischer, R.; Langer, J. *Angew. Chem., Int. Ed.* **2007**, *46*, 1950. (e) Krieck, S.; Gorls, H.; Yu, L.; Reiher, M.; Westerhausen, M. *J. Am. Chem. Soc.* **2009**, *131*, 2977.

(4) (a) Vargas, W.; Englich, U.; Ruhlandt-Senge, K. *Inorg. Chem.* **2002**, *41*, 5602. (b) Alexander, J. S.; Ruhlandt-Senge, K. *Eur. J. Inorg. Chem.* **2002**, 2761. (c) Hitzbleck, J.; O'Brien, A. Y.; Forsyth, C. M.; Deacon, G. B.; Ruhlandt-Senge, K. *Chem. Eur. J.* **2004**, *10*, 3315. (d) Gillett-Kunnath, M.; Teng, W.; Vargas, W.; Ruhlandt-Senge, K. *Inorg. Chem.* **2005**, *44*, 4862. (e) Torvisco, A.; Decker, K.; Uhlig, F.; Ruhlandt-Senge, K. *Inorg. Chem.* **2009**, *48*, 11459. (f) Torvisco, A.; O'Brien, A. Y.; Ruhlandt-Senge, K. *Coord. Chem. Rev.* **2011**, *255*, 1268.

(5) (a) Ruspic, C.; Nembenna, S.; Hofmeister, A.; Magull, J.; Harder, S.; Roesky, H. W. *J. Am. Chem. Soc.* **2006**, *128*, 15000. (b) Nembenna, S.; Roesky, H. W.; Nagendran, S.; Hofmeister, A.; Magull, J.; Wilbrandt, P.-J.; Hahn, M. *Angew. Chem., Int. Ed.* **2007**, *46*, 2512. (c) Pillai Sarish, S.; Jana, A.; Roesky, H. W.; Schulz, T.; John, M.; Stalke, D. *Inorg. Chem.* **2010**, *49*, 3816.

(6) (a) Harder, S.; Brettar, J. *Angew. Chem., Int. Ed.* **2006**, *45*, 3474. (b) Ruspic, C.; Harder, S. *Inorg. Chem.* **2007**, *46*, 10426. (c) Spielmann, J.; Buch, F.; Harder, S. *Angew. Chem., Int. Ed.* **2008**, *47*, 9434. (d) Spielmann, J.; Harder, S. *J. Am. Chem. Soc.* **2009**, *131*, 5064.

(7) (a) Crimmin, M. R.; Casely, I. J.; Hill, M. S. *J. Am. Chem. Soc.* **2005**, *127*, 2042. (b) Crimmin, M. R.; Barrett, A. G. M.; Hill, M. S.; Hitchcock, P. B.; Procopiou, P. A. *Organometallics* **2007**, *26*, 2953. (c) Crimmin, M. R.; Arrowsmith, M.; Barrett, A. G. M.; Casely, I. J.; Hill, M. S.; Procopiou, P. A. *J. Am. Chem. Soc.* **2009**, *131*, 9670. (d) Liptrot, D. J.; Hill, M. S.; Mahon, M. F.; MacDougall, D. J. *Chem. Eur. J.* **2010**, *16*, 8508. (e) Brinkmann, C.; Barrett, A. G. M.; Hill, M. S.; Procopiou, P. A. *J. Am. Chem. Soc.* **2012**, *134*, 2193.

(8) (a) Buchanan, W. D.; Allis, D. G.; Ruhlandt-Senge, K. *Chem. Commun.* **2010**, *46*, 4449. For a recent illustration, see: (b) Loh, C.; Seupel, S.; Görls, H.; Krieck, S.; Westerhausen, M. *Organometallics* **2014**, *33*, 1480.

(9) (a) Sarazin, Y.; Roşca, D.-A.; Poirier, V.; Roisnel, T.; Silvestru, A.; Maron, L.; Carpentier, J.-F. *Organometallics* **2010**, *29*, 6569. (b) Michel, O.; Törnroos, K. W.; Maichle-Mössmer, C.; Anwander, R. *Chem. Eur. J.* **2011**, *17*, 4964. (c) Michel, O.; Törnroos, K. W.; Maichle-Mössmer, C.; Anwander, R. *Eur. J. Inorg. Chem.* **2012**, 44.

(10) (a) Liu, B.; Roisnel, T.; Carpentier, J.-F.; Sarazin, Y. *Chem. Eur. J.* **2013**, *19*, 2784. (b) Hill, M. S.; Liptrot, D. J.; MacDougall, D. J.; Mahon, M. F.; Robinson, T. P. *Chem. Sci.* **2013**, *4*, 4212.

(11) (a) Buchanan, W. D.; Guino-o, M. A.; Ruhlandt-Senge, K. *Inorg. Chem.* **2010**, *49*, 7144. (b) Buchanan, W. D.; Ruhlandt-Senge, K. *Chem. Eur. J.* **2013**, *19*, 10708.

(12) (a) Lavanant, L.; Chou, T.-Y.; Chi, Y.; Lehmann, C. W.; Toupet, L.; Carpentier, J.-F. *Organometallics* **2004**, *23*, 5450. (b) Carpentier, J.-F. *Dalton Trans.* **2010**, *39*, 37 and references cited therein. (c) Bouyahyi, M.; Roisnel, T.; Carpentier, J.-F. *Organometallics* **2010**, *29*, 491. (d) Dagorne, S.; Bouyahyi, M.; Vergnaud, J.; Carpentier, J.-F. *Organometallics* **2010**, *29*, 1865. (e) Bouyahyi, M.; Roisnel, T.; Carpentier, J.-F. *Organometallics* **2012**, *31*, 1458. (f) Normand, M.; Kirillov, E.; Roisnel, T.; Carpentier, J.-F. *Organometallics* **2012**, *31*, 1448.

(13) Sarazin, Y.; Liu, B.; Roisnel, T.; Maron, L.; Carpentier, J.-F. *J. Am. Chem. Soc.* **2011**, *133*, 9069.

(14) Like $\{RO_0^F\}H$,[13] the protio ligands $\{RO_2^F\}H$ and $\{RO_3^F\}H$ are isolated as colorless oils. On the other hand, $\{RO_1^F\}H$ is a crystalline material, and its molecular solid-state structure was elucidated. See the Supporting Information for details.

(15) The protio ligand $\{RO_2^F\}H$ was first employed by Chi and coworkers for the synthesis of the homoleptic compounds $\{RO_2^F\}_2Ae$ (Ae = Sr, Ca), which act as potent source reagents for the chemical vapor deposition of SrF_2 and BaF_2 thin films: Chi, Y.; Ranjan, S.; Chou, T.-Y.; Liu, C.-S.; Peng, S.-M.; Lee, G.-H. *Dalton Trans.* **2001**, 2462.

(16) Lum, J. S.; Tahsini, L.; Golen, J. A.; Moore, C.; Rheingold, A. L.; Doerrer, L. H. *Chem. Eur. J.* **2013**, *19*, 6374.

(17) Kawashima, T.; Iwama, N.; Tokitoh, N.; Okazaki, R. *J. Org. Chem.* **1994**, *59*, 491.

(18) Snelgrove, J.; Fogg, D. Private communication, CCDC No. 183980.

(19) Guillemot, G.; Solari, E.; Rizzoli, C.; Floriani, C. *Chem. Eur. J.* **2002**, *8*, 2072.

(20) (a) Chisholm, M. H.; Drake, S. R.; Naiini, A. A.; Streib, W. E. *Polyhedron* **1991**, *10*, 337. (b) Samuels, J. A.; Folting, K.; Huffman, J. C.; Caulton, K. G. *Chem. Mater.* **1995**, *7*, 929.

(21) The minimum and maximum distances for K···F interactions were defined by Plenio as 2.98 and 3.47 Å: Plenio, H. *Chem. Rev.* **1997**, *97*, 3363. They correspond respectively to the sum of the ionic radius of potassium (1.51 Å) and the van der Waals radius of fluorine (1.47 Å), and the sum of the van der Waals radii of fluorine and the ionic van der Waals radii of potassium by Kollman. As the maximum tolerated distance seemed excessive to us in view of recent examples available from the CCDC database, we have set it as the average of the

minimum and maximum distances defined by Plenio, even if we are aware that this may be somewhat restrictive.
(22) The limit for Ca···F interactions was set at 3.13 Å, as recommended by Plenio.[21]
(23) Barrett, A. G. M.; Crimmin, M. R.; Hill, M. S.; Hitchcock, P. B.; Procopiou, P. A. *Angew. Chem., Int. Ed.* **2007**, *46*, 6339.
(24) (a) Roşca, S.-C.; Roşca, D.-A.; Dorcet, V.; Kozak, C. M.; Kerton, F. M.; Carpentier, J.-F.; Sarazin, Y. *Dalton Trans.* **2013**, *42*, 9361. For other examples with zinc or yttrium, see: (b) Williams, C. K.; Breyfogle, L. E.; Kyung Choi, S.; Nam, W.; Young, V. G., Jr.; Hillmyer, M. A.; Tolman, W. B. *J. Am. Chem. Soc.* **2003**, *125*, 11350. (c) Platel, R. H.; Hodgson, L. M.; White, A. J. P.; Williams, C. K. *Organometallics* **2007**, *26*, 4955.
(25) Measurements for $[\{RO_1^F\}K]_2$ ($[\mathbf{1}]_2$) could not be performed in benzene-d_6 owing to the poor solubility of the complex in this solvent. The diffusion coefficient ($D_t = 3.60 \times 10^{-9}$ m^2 s^{-1}) measured in dichloromethane-d_2 shows that the complex remains dimeric in this solvent ($r_{H,PGSE} = 5.66$ Å, $r_{H,X\text{-}ray} = 5.04$ Å).
(26) The following values were determined for TMSS (considered spherical): $D_t^{TMSS,benzene\text{-}d6} = (1.0750-1.8430) \times 10^{-9}$ m^2 s^{-1} (depending on the concentration ot TMSS that was used) and $c^{TMSS,\ benzene\text{-}d6} = 4.8223$ Å, using $f^{TMSS} = 1.00$ and $r_H^{TMSS} = 4.28$ Å. The value of $c^{TMSS,benzene\text{-}d_6}$ was calculated according to $c^{TMSS} = (6/(1 + 0.695)(r_H^{solv}/r_H^{TMSS})^{2.234})$ using $r_H^{benzene\text{-}d_6} = 2.68$ Å as found in: Zuccaccia, D.; Macchioni, A. *Organometallics* **2005**, *24*, 3476.
(27) Partial or total decomposition to $\{RO_x^F\}_2Ca$ and $Ca(N(SiMe_3)_2)_2$ would have resulted in the detection of three and two clearly distinct diffusion coefficients, respectively.
(28) Brown, I. D.; Altermatt, D. *Acta Crystallogr. Sect. B* **1985**, *B41*, 244.
(29) Brese, N. E.; O'Keefe, M. *Acta Crystallogr., Sect. B* **1991**, *B47*, 192.
(30) Sum, J. S.; Tahsini, L.; Golen, J. A.; Moore, C.; Rheingold, A. L.; Doerrer, L. H. *Chem. Eur. J.* **2013**, *19*, 6374.
(31) Lancaster, S. J.; Rodriguez, A.; Lara-Sanchez, A.; Hannant, M. D.; Walker, D. A.; Hughes, D. L.; Bochmann, M. *Organometallics* **2002**, *21*, 451.
(32) Hannant, M. H.; Wright, J. A.; Lancaster, S. J.; Hughes, D. L.; Horton, P. N.; Bochmann, M. *Dalton Trans.* **2006**, 2415.
(33) Bochmann, M. *Coord. Chem. Rev.* **2009**, *253*, 2000.
(34) These crystals were grown by recrystallization from saturated dichloromethane (moisture level <5 ppm) solutions prepared and stored in a glovebox with a moisture level lower than 4 ppm. Crystallization outside the glovebox and/or using silylated glassware or Teflon vials gave the same outcome.
(35) Hu, H.; Cui, C. *Organometallics* **2012**, *31*, 1208.
(36) (a) Liu, B.; Roisnel, T.; Carpentier, J.-F.; Sarazin, Y. *Angew. Chem., Int. Ed.* **2012**, *51*, 4943. (b) Liu, B.; Roisnel, T.; Carpentier, J.-F.; Sarazin, Y. *Chem. Eur. J.* **2013**, *19*, 13445.
(37) Koshti, V.; Gaikwad, S.; Chikkali, S. H. *Coord. Chem. Rev.* **2014**, *265*, 52.
(38) (a) Zulys, A.; Dochnahl, M.; Hollmann, D.; Löhnwitz, K.; Herrmann, J.-S.; Roesky, P. W.; Blechert, S. *Angew. Chem., Int. Ed.* **2005**, *44*, 7794. (b) Dochnahl, M.; Löhnwitz, K.; Pissarek, J.-W.; Biyikal, M.; Schulz, S. R.; Schön, S.; Meyer, N.; Roesky, P. W.; Blechert, S. *Chem. Eur. J.* **2007**, *13*, 6654.
(39) He, X.; Noll, B. C.; Beatty, A.; Mulvey, R. E.; Henderson, K. W. *J. Am. Chem. Soc.* **2004**, *126*, 7444.
(40) Boncella, J. M.; Coston, C. J.; Cammack, J. K. *Polyhedron* **1991**, *10*, 769.